

Institute of Fundamental Technological Research,
Polish Academy of Sciences (IPPT PAN)
Warsaw, 5th December 2007

Multi-Scale Simulations of Coupled Fluid Flow and Electromagnetism: From Origins of Planetary Magnetic Fields to Improved Cancer Therapy

S. Kenjeres*

*Department of Multi Scale Physics and J.M. Burgers Centre for Fluid Mechanics
Faculty of Applied Sciences, Delft University of Technology*

5 December 2007

1



* **Royal Netherlands Academy of Arts and Sciences (KNAW) research fellow (2001-2006)**

J.M. Burgerscentrum





-MagnetoHydrodynamics (MHD): electrically conductive fluid flow/electromagnetic fields interactions

-MHD interactions play the key role in many physical phenomena:

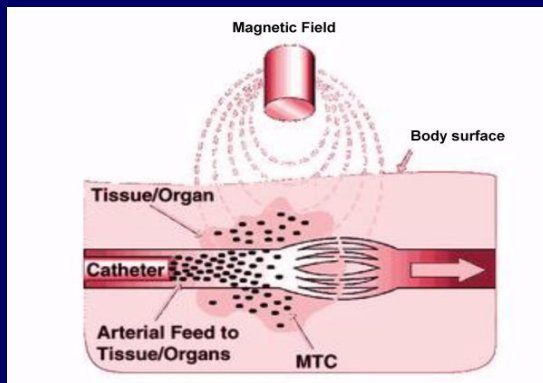
Continuous steel-casting



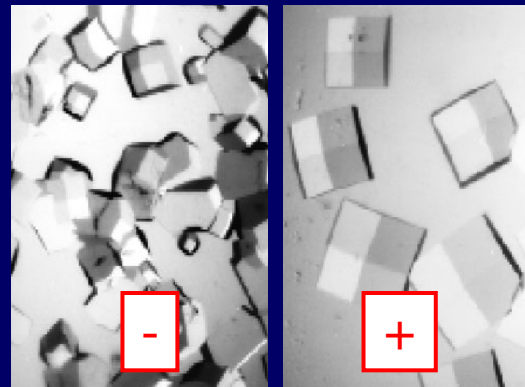
Aluminium reduction cells



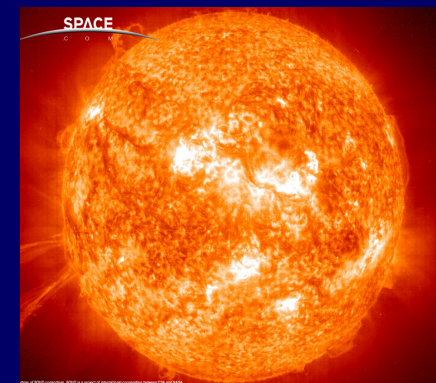
Magnetic Drug Delivery



Crystal growth

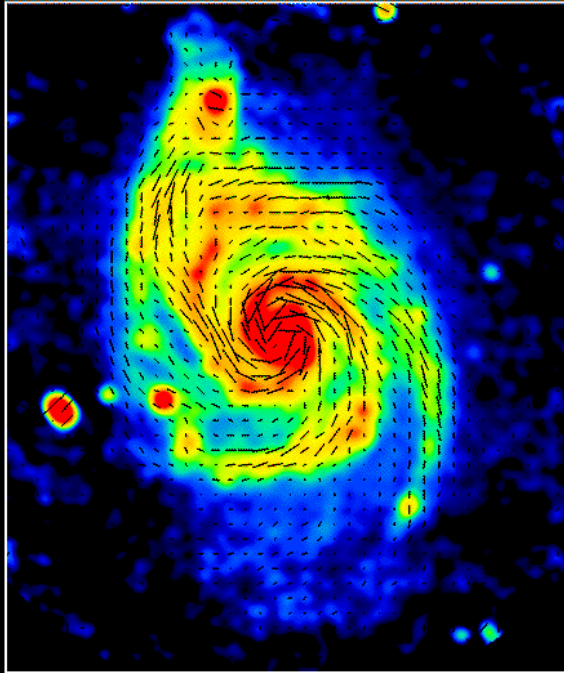


Geo- and Astro-physics



-Immense variety of scales: from spiral galaxies to electro-magnetically driven mini tornados

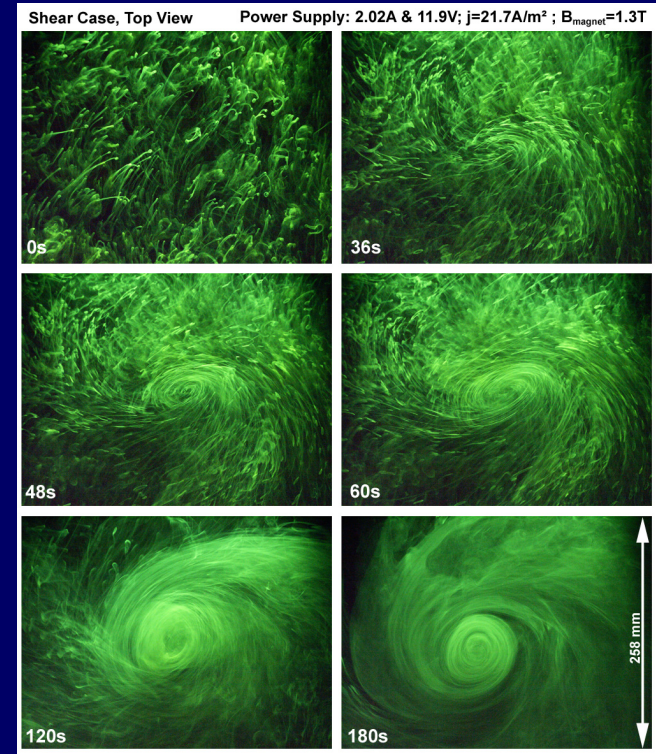
M51 6cm Total Intensity+Magnetic Field (VLA+Effelsberg)



Copyright: MPIR, Bonn (B.Beck, C.Horellou & N.Neisinger)

-astronomical observations:

background magnetic field inside M51 galaxy, Beck *et al.* (2000)



-laboratory observations:

PLIF and PIV measurements, Verdoold *et al.* (2004)

2 permanent magnets + 2 electrodes

(perpendicular to each other)

Characteristic Dimensionless MHD Parameters

Reynolds number

$$Re = \frac{U \cdot D}{\nu}$$

Inertia/Viscous forces

Magnetic Reynolds number

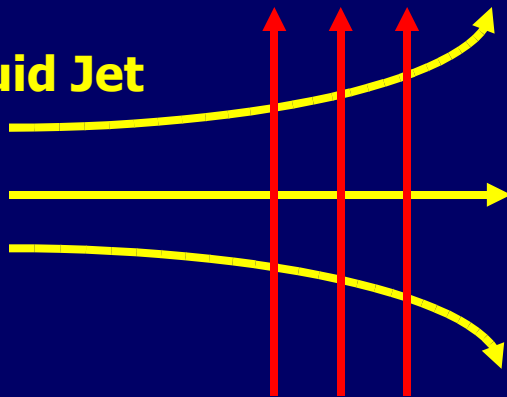
$$Re_m = \frac{t_d}{t_k} = \frac{\mu_0 \sigma D^2}{D/U} = \mu_0 \sigma U D$$

Stretching/Resistive dumping

-Magnetic Dynamo:

the process of partial conversion of the **mechanical energy** of a moving electrically conductive medium into the **magnetic energy!**

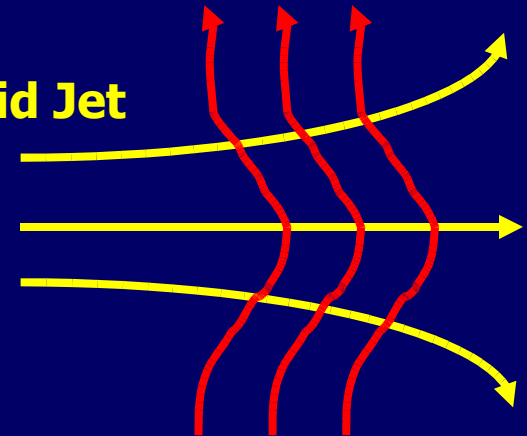
Fluid Jet



Magnetic Field

$$Re_m \ll 1$$

Fluid Jet

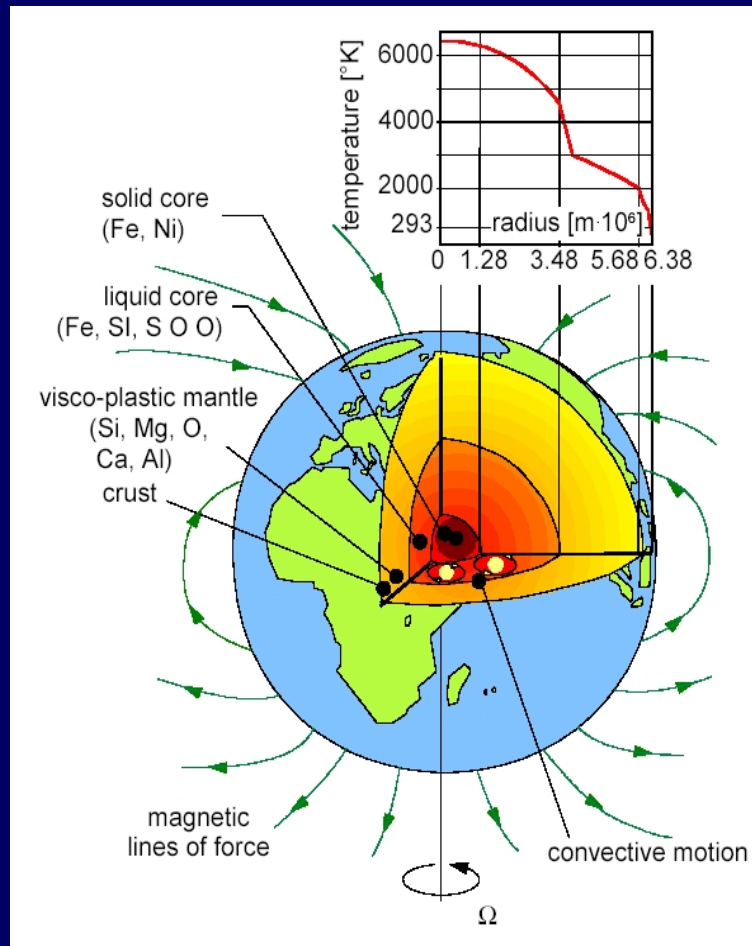


$$Re_m > 1$$

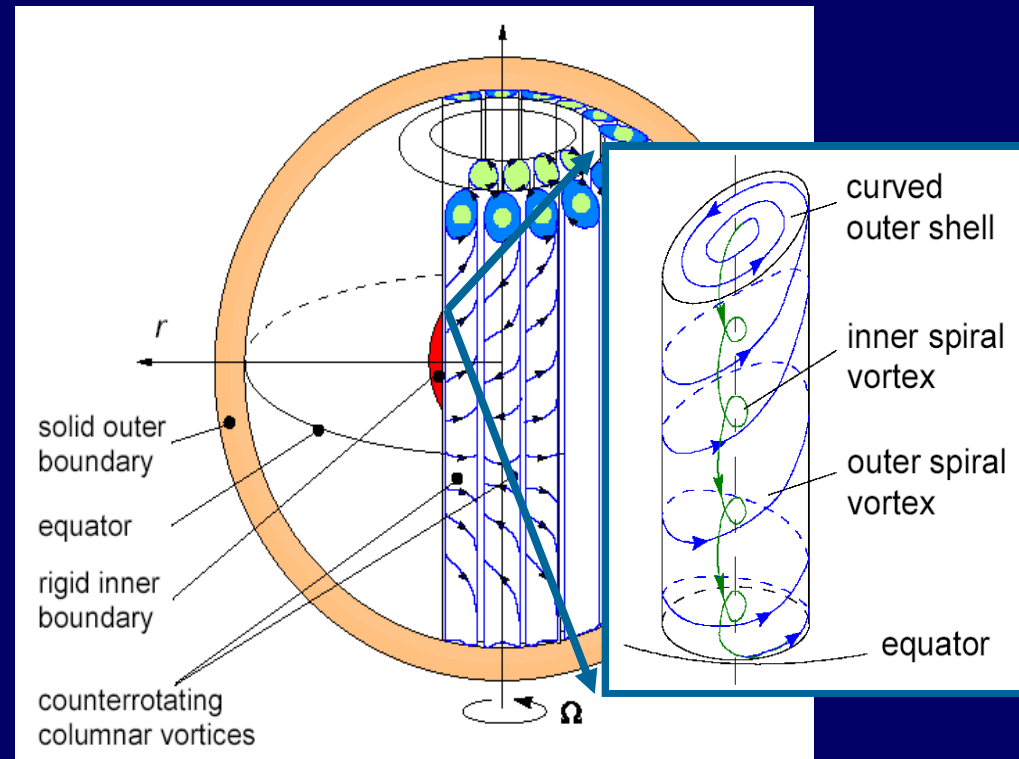
Magnetic Field

Magnetic-Dynamo Condition: $Re_m > 1$!

Dynamo principle demonstration: geo-dynamo theory



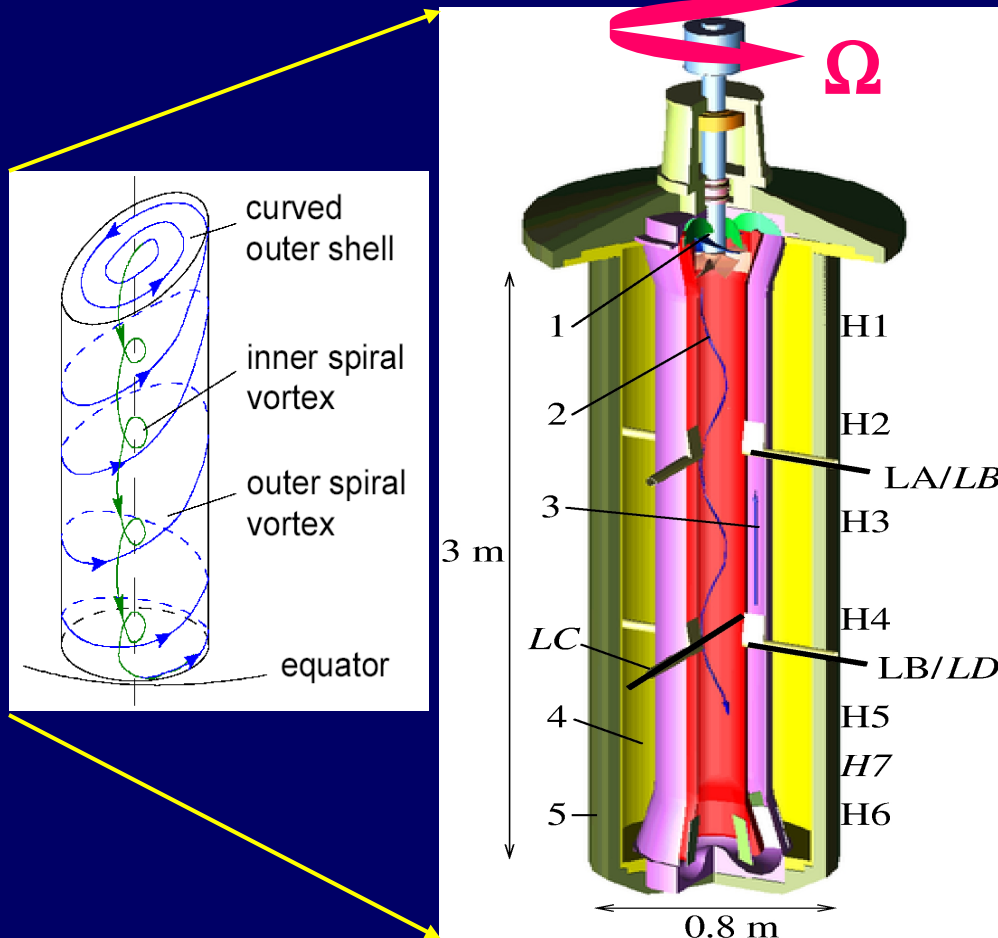
**-Structure of the Earth,
Beatty and Chaikin (1990)**



**-Columnar vortex pattern of convection in
rotating sphere, Busse (1994)**

Laboratory studies based on the Riga dynamo facilities

Gailitis *et al.* (1967,...,2004), Institute of Physics, University of Latvia



1. Impeller

2. Helical flow region

3. Back-flow region

4. Sodium at rest

5. Stainless steel container

H1...H7 – Hall probe sensors

$Re=3.5 \times 10^6$

$Re_m=10-30$

$Pr_m=6.5 \times 10^{-6}$

Sodium at 150°C, pump with 2x110 kW power !!

Momentum + Magnetic Induction → Continuum Unifying Principles

$$\dots F_i^R = 2\varepsilon_{ijk} U_j \Omega_k \quad F_i^L = \varepsilon_{ijk} J_j B_k$$

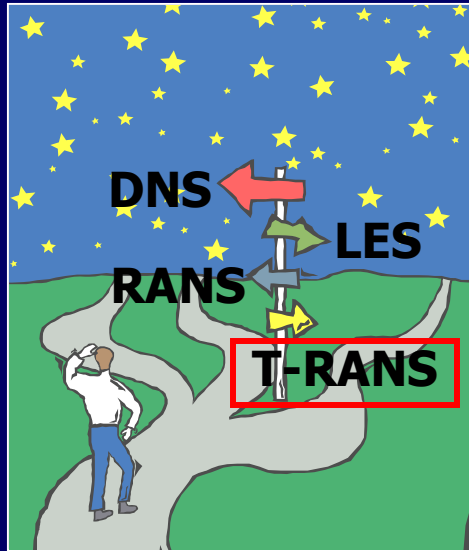
$$\frac{\partial U_i}{\partial t} + U_j \frac{\partial U_i}{\partial x_j} = -\frac{\partial P}{\partial x_i} + \frac{\partial}{\partial x_j} \left[\nu \left(\frac{\partial U_i}{\partial x_j} + \frac{\partial U_j}{\partial x_i} \right) \right] + \frac{1}{\rho} \sum F_i$$

$$\frac{\partial B_i}{\partial t} + U_j \frac{\partial B_i}{\partial x_j} = \frac{1}{\mu_0 \sigma} \frac{\partial^2 B_i}{\partial x_j^2} + B_j \frac{\partial U_i}{\partial x_j}$$

+ divergence free conditions:

$$\frac{\partial U_i}{\partial x_i} = 0 \quad \frac{\partial B_i}{\partial x_i} = 0$$

Modelling/Simulation Approach → Hybrid T-RANS (N-S) / DNS (Maxwell)



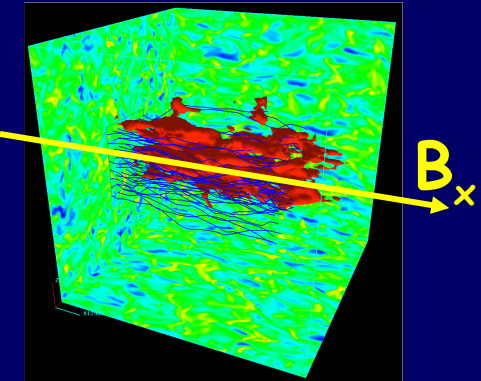
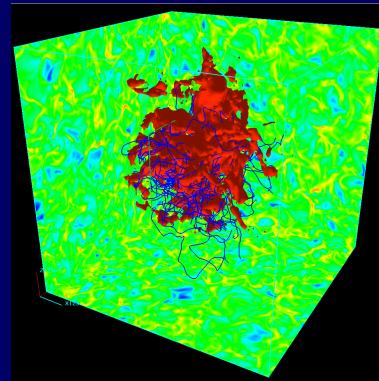
Advanced subscale/subgrid turbulence modelling

high Re , Re_m , Ha

Body force: strong anisotropy of turbulence

Wall effects: viscous + blockage, low- Re

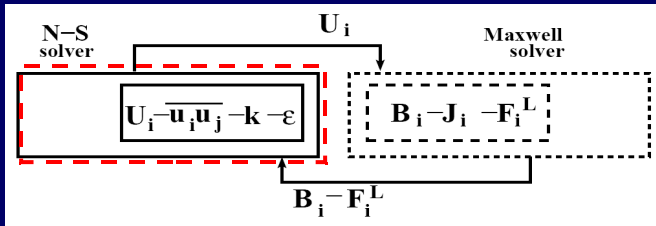
MHD turbulence



$$\langle u_i u_j \rangle$$

$$F_i^L \longrightarrow \langle U_i \rangle \quad f_i^L \longrightarrow u_i$$

Modelling/Simulation Approach → Hybrid T-RANS (N-S) / DNS (Maxwell)



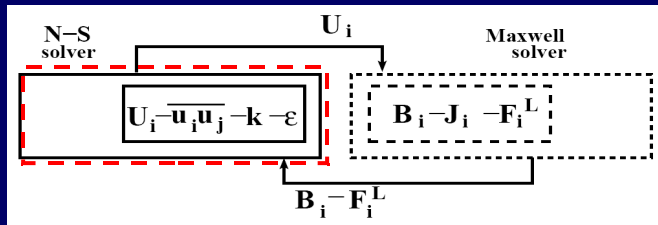
(1) Source/sink terms (production/destruction)

$$S_{ij}^M = \frac{\sigma}{\rho} \left(\begin{array}{l} \boxed{\epsilon_{imn} B_n \overline{e_m u_j} + \epsilon_{jmn} B_n \overline{e_m u_i}} + B_i B_n \overline{u_j u_n} \\ + B_j B_n \overline{u_i u_n} - 2 B_n B_n \overline{u_i u_j} \end{array} \right)$$

(2) Redistributive mechanism

$$\frac{\partial^2 p}{\partial x_l^2} = - \frac{\partial^2}{\partial x_l \partial x_m} \left(\rho u_l u_m - \rho \overline{u_l u_m} \right) - 2 \rho \frac{\partial U_l}{\partial x_m} \frac{\partial u_m}{\partial x_l} + \rho \frac{\partial f_i}{\partial x_i}$$

Modelling/Simulation Approach → Hybrid T-RANS (N-S) / DNS (Maxwell)



(3) T-RANS subscale Second Moment Closure

$$\frac{\partial \overline{u_i u_j}}{\partial t} + U_l \frac{\partial \overline{u_i u_j}}{\partial x_l} = \frac{\partial}{\partial x_l} \left[\left(\nu \delta_{lm} + C_s \frac{k}{\varepsilon} \overline{u_l u_m} \right) \frac{\partial \overline{u_i u_j}}{\partial x_m} \right] + P_{ij} + \Phi_{ij}^S + \Phi_{ij}^R + \Phi_{ij}^M - \varepsilon_{ij} + S_{ij}^M \quad (7)$$

Speziale, Sarkar, Gatski (1991)
+
Kenjeres and Hanjalic
(2001,2004,2005)

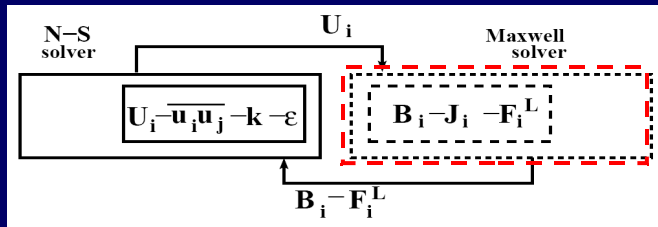
$$S_{ij}^M = S_{ij}^{M1} + S_{ij}^{M2}$$

$$S_{ij}^{M1} = -\frac{\sigma}{\rho} \left(\epsilon_{ilm} B_m \overline{u_j \frac{\partial \varphi}{\partial x_l}} + \epsilon_{jlm} B_m \overline{u_i \frac{\partial \varphi}{\partial x_l}} \right)$$

$$S_{ij}^{M2} = \frac{\sigma}{\rho} (B_i B_l \overline{u_j u_l} + B_j B_l \overline{u_i u_l} - 2B_l^2 \overline{u_i u_j})$$

$$\overline{u_i \frac{\partial \varphi}{\partial x_j}} = C_\lambda \epsilon_{jlm} B_m \overline{u_i u_l}$$

Modelling/Simulation Approach → Hybrid T-RANS (N-S) / DNS (Maxwell)



(4) DNS for magnetic induction equations

$$Re_m = 10-30$$

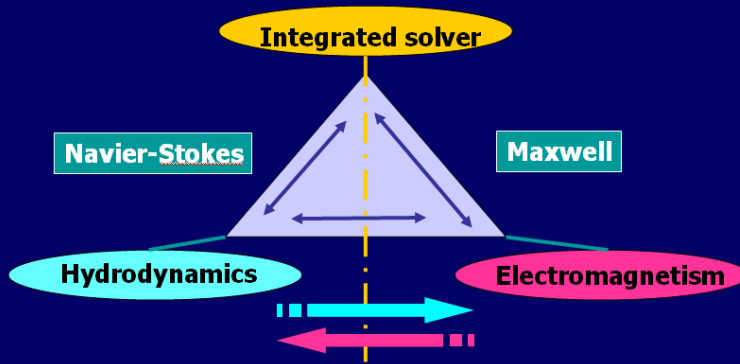
$$Pr_m = 6.5 \times 10^{-6}$$

$$\left. \begin{aligned} \eta_U &= \left(\nu^3 / \epsilon \right)^{1/4} \\ \eta_B &= \left(\lambda^3 / \epsilon \right)^{1/4} \end{aligned} \right\} \rightarrow \eta_U / \eta_B = Pr_m^{3/4}$$

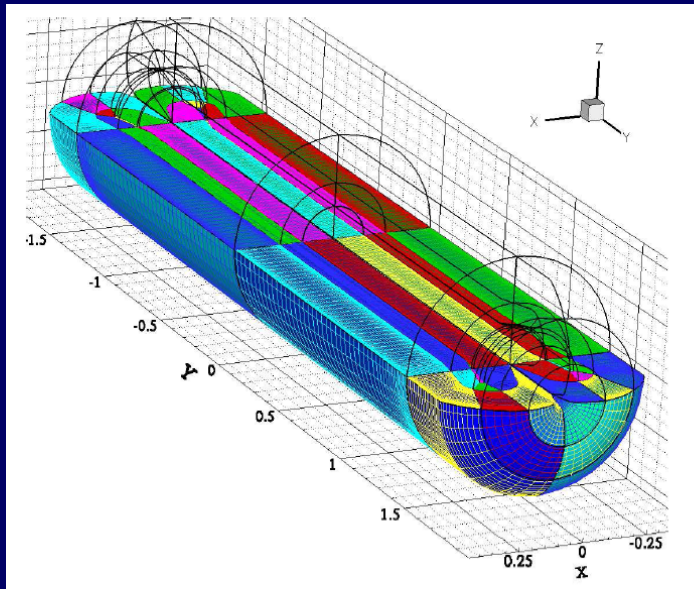
-Magnetic diffusive length scales \gg velocity viscous scales

-Experimentally observed frequencies of magnetic field ~ 1 Hz

Numerical Solver and Computational Mesh

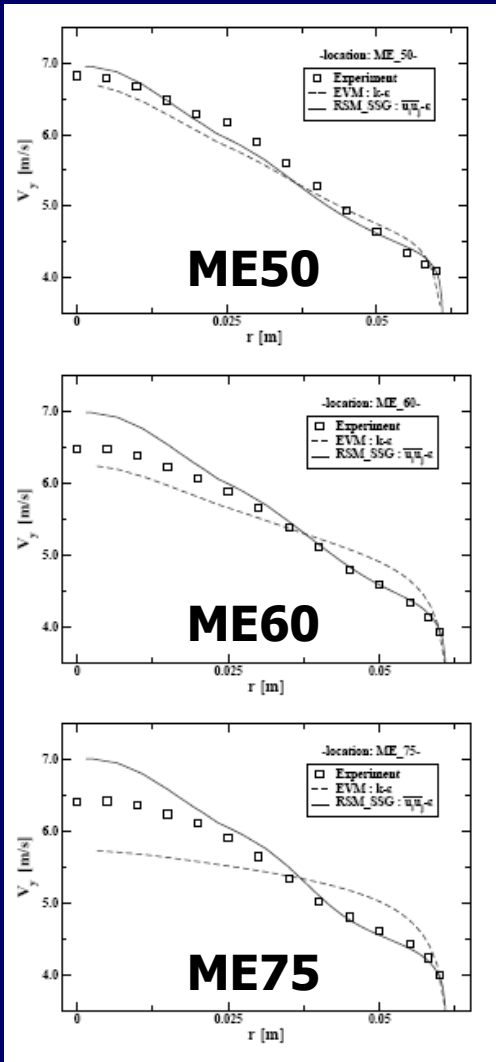


- Finite volume second-order for the non-orthogonal multi-domain/multi-block
- TVD (UMIST limiter) for convective terms
- CDS for diffusive terms
- fully implicit three-time steps integration
- MPI (32-128 CPUs) SGI-Altix

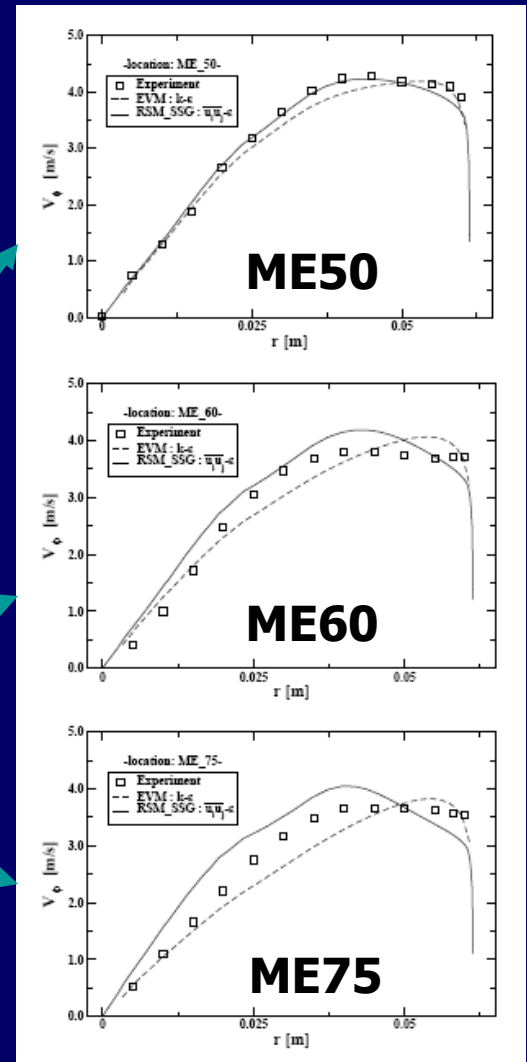
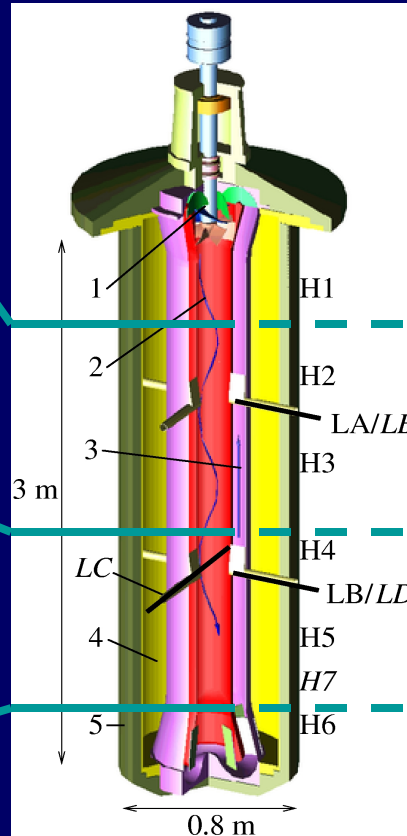


- Numerical mesh: 90 multi-blocks with $\sim 4 \times 10^6$ CVs
- Wall-functions for velocity and turbulence variables $45 < (x^+, z^+) < 100$
- Vertical magnetic field condition in order to allow natural escape of self-generated magnetic field
- Time step: $\Delta t \sim 1/100$ of the experimentally observed periods

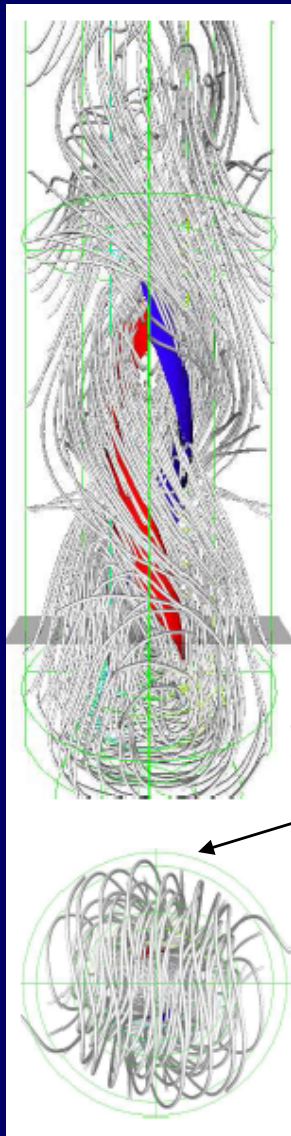
-1:2 water model-



-axial velocity-

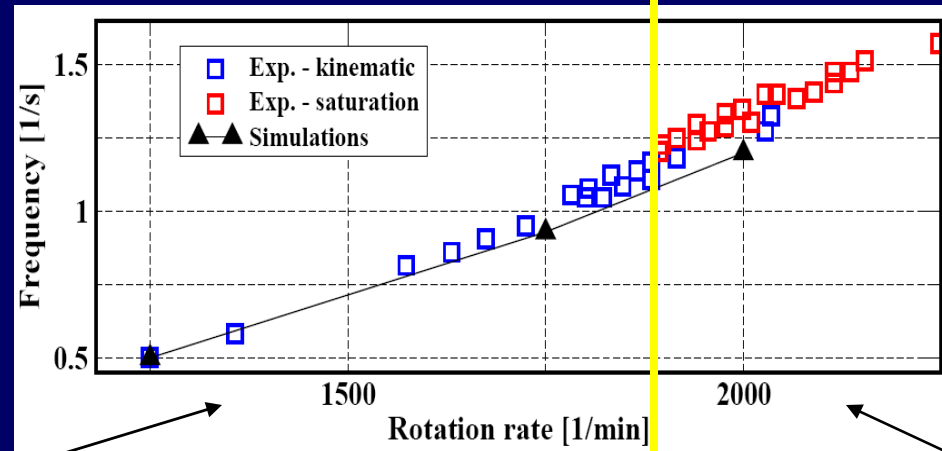


-tangential velocity-

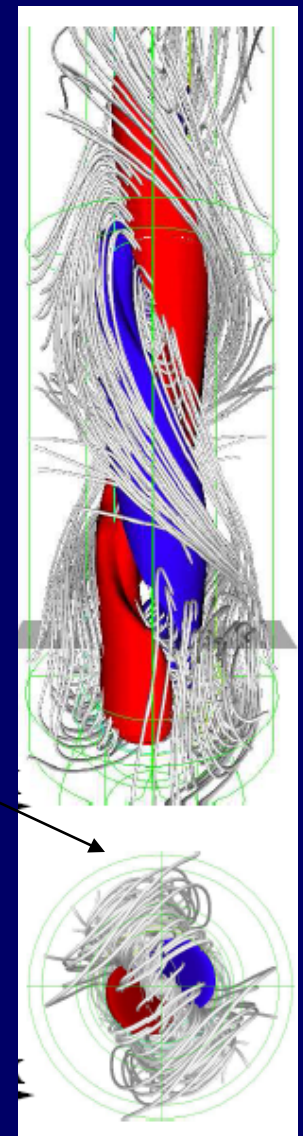


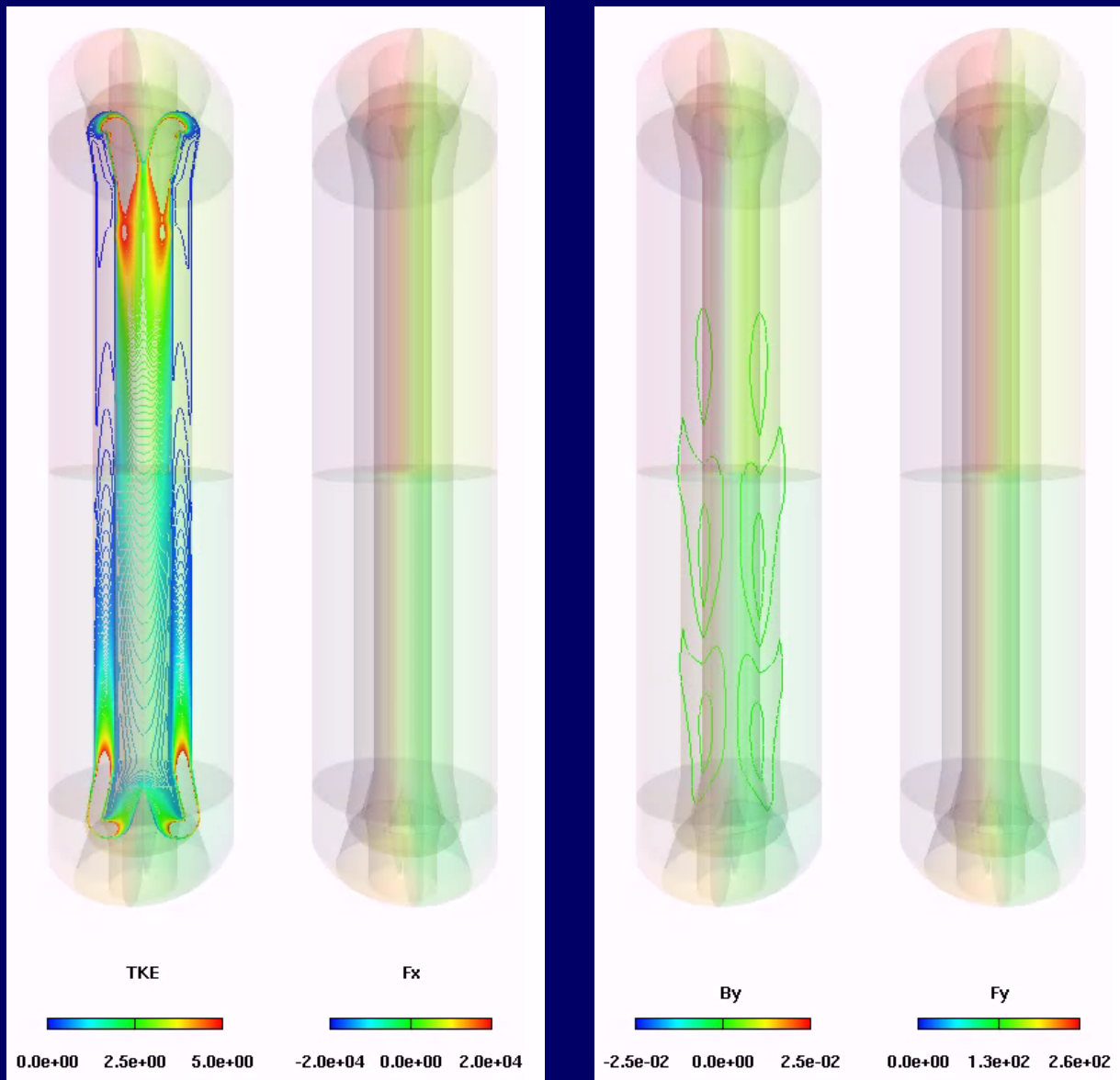
**-kinematic-
(one-way)**

**-saturation-
(two-way)**



**-Frequency versus rotation rate:
comparison with experiments with
sodium as working fluid -**



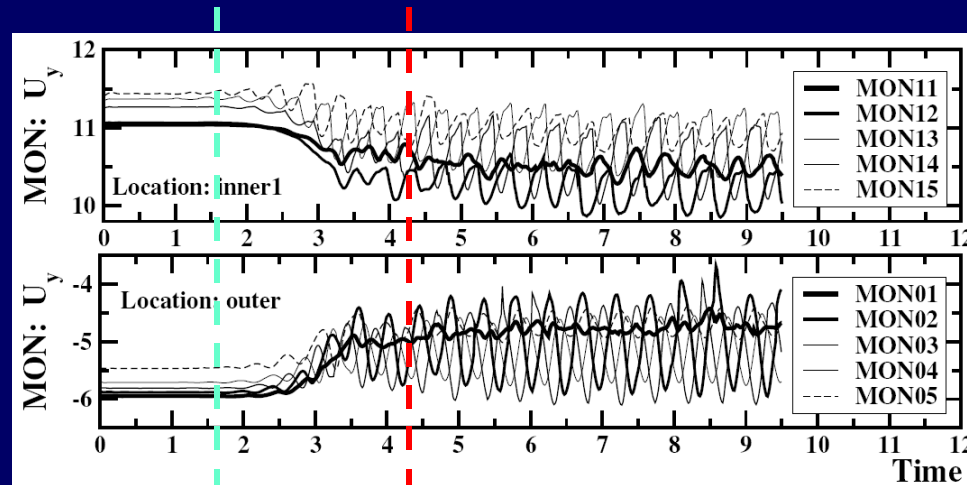


5 December 2007

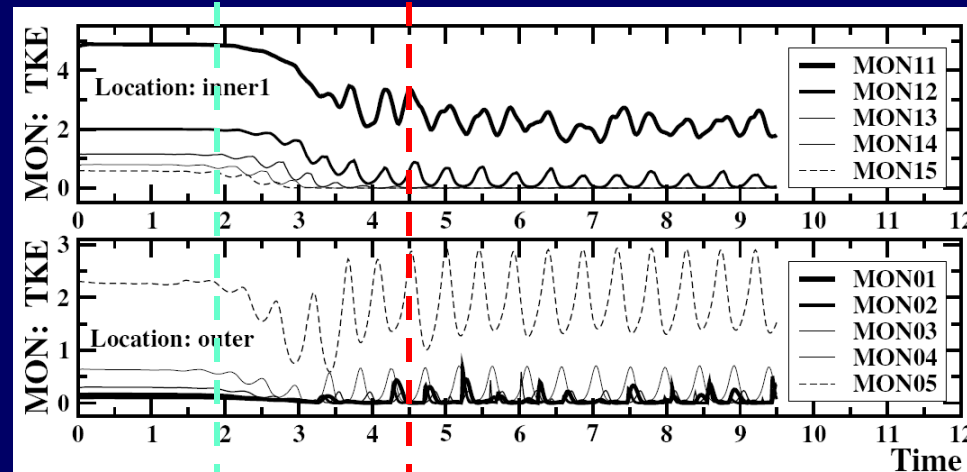
15

Time evolutions in the central vertical plane: TKE-Fx, By-Fy (axial) \sim 6.5 sec of real time.

Time Evolutions of Axial Velocity and TKE



$U_y \rightarrow$ suppressed

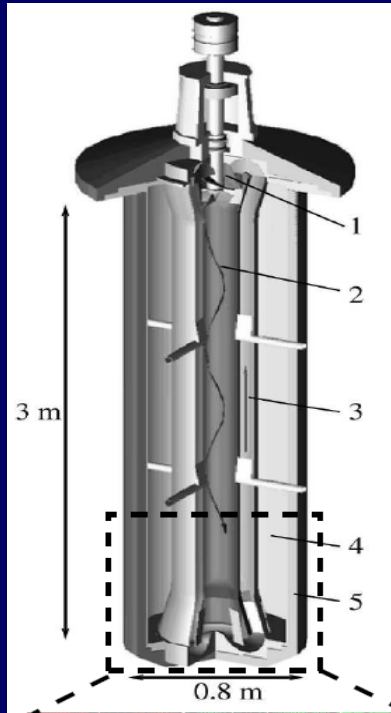


TKE \rightarrow suppressed

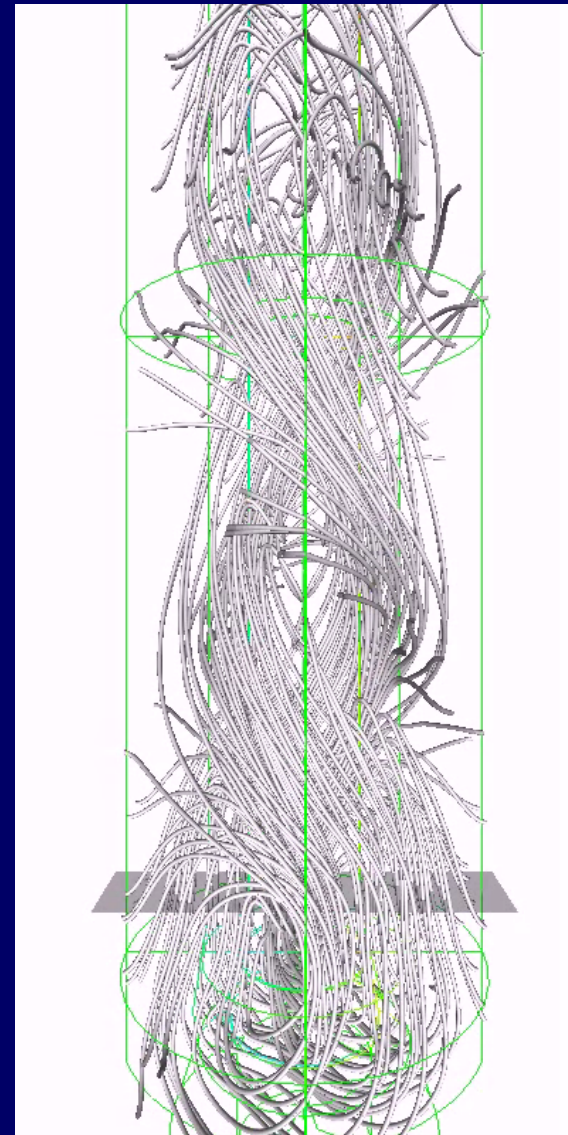
TKE \rightarrow enhanced

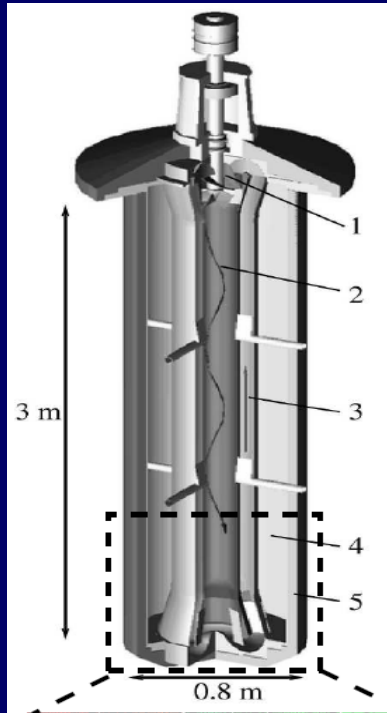
kinematic (one-way)

saturation (two-way)

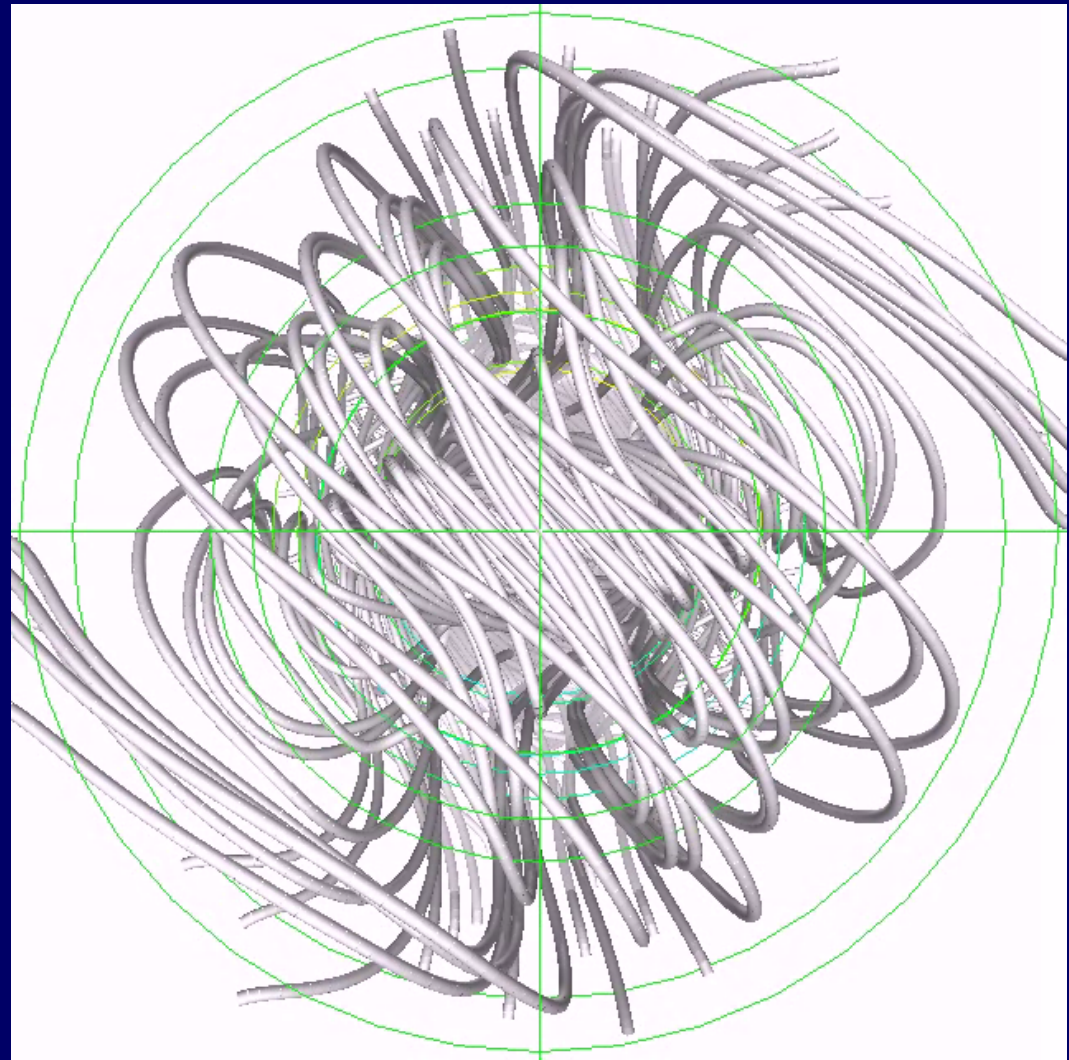


-view from side-

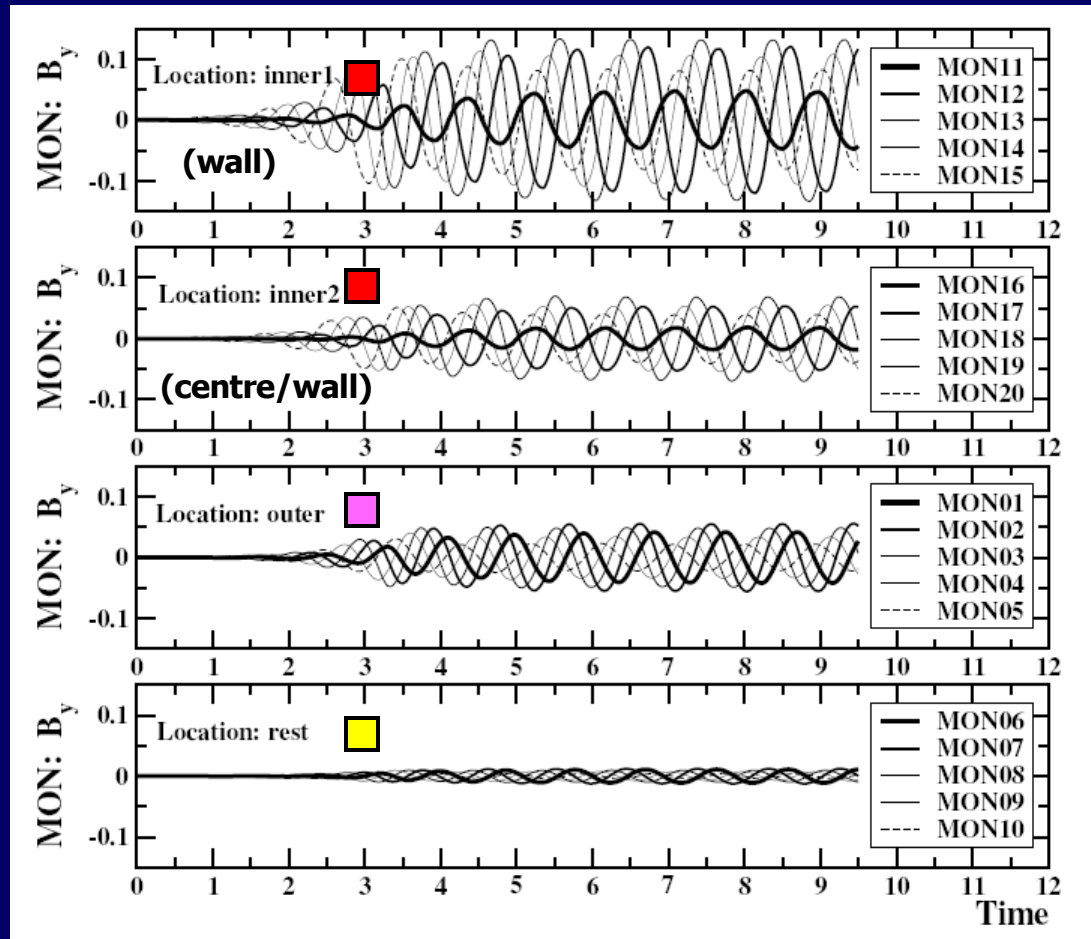
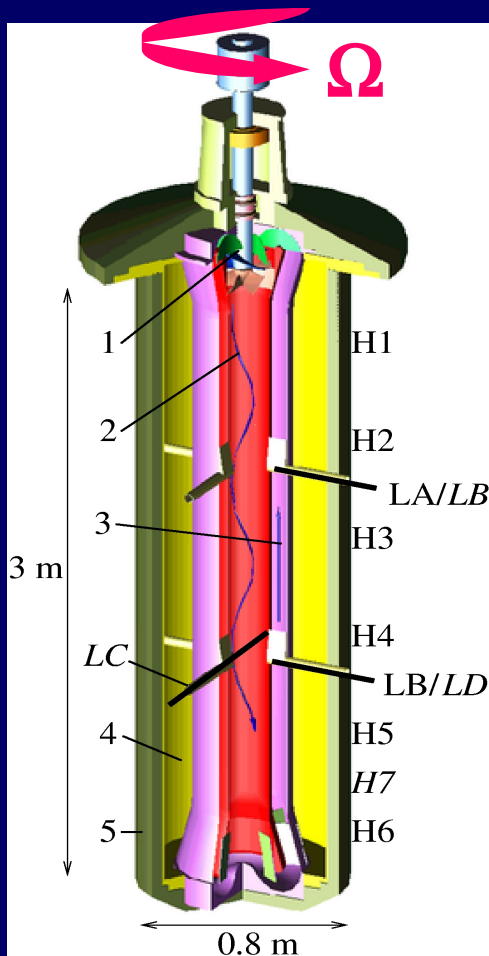




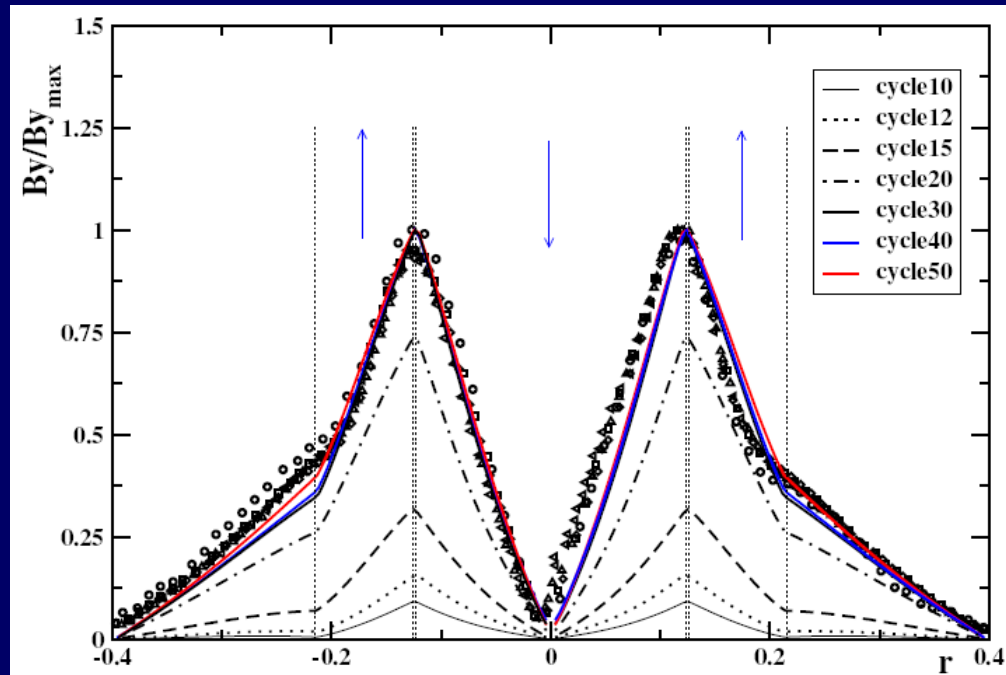
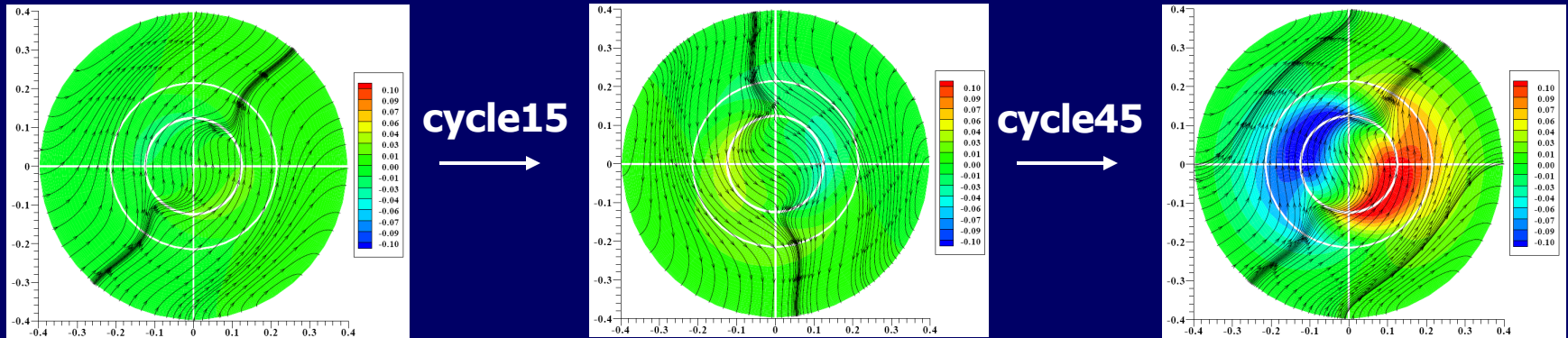
-view from below-



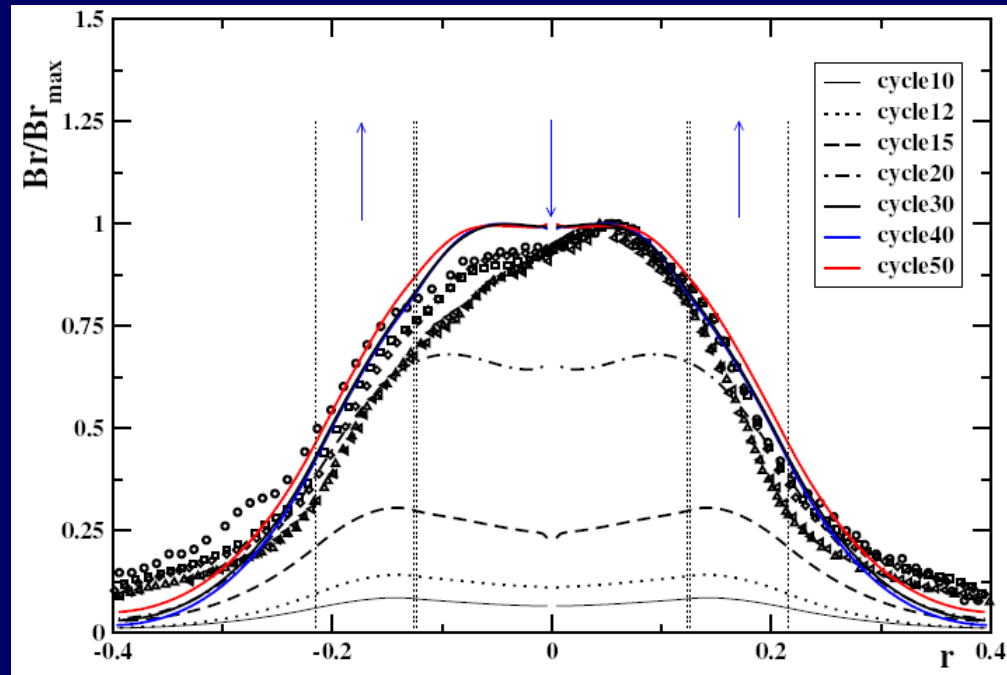
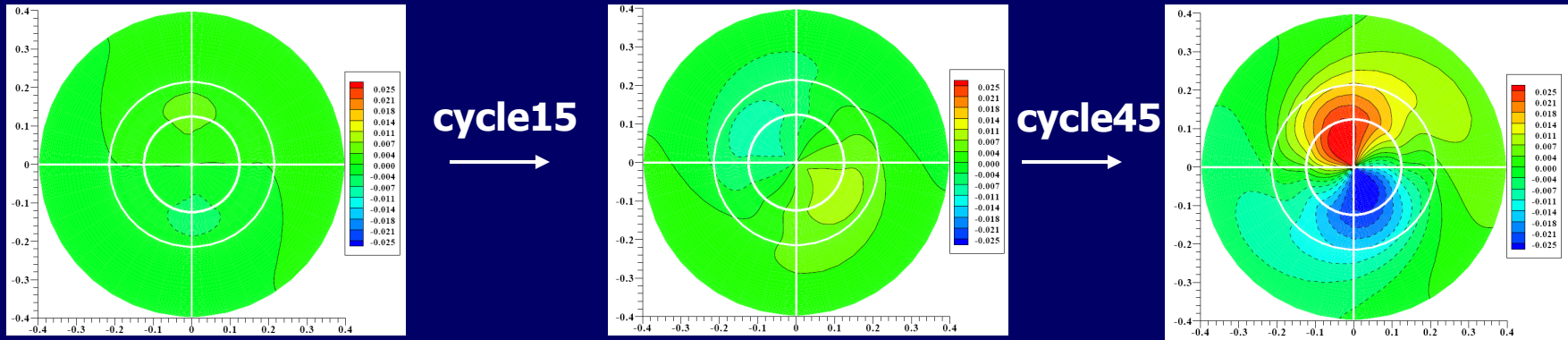
Time Evolutions of Self-Generated Magnetic Fields



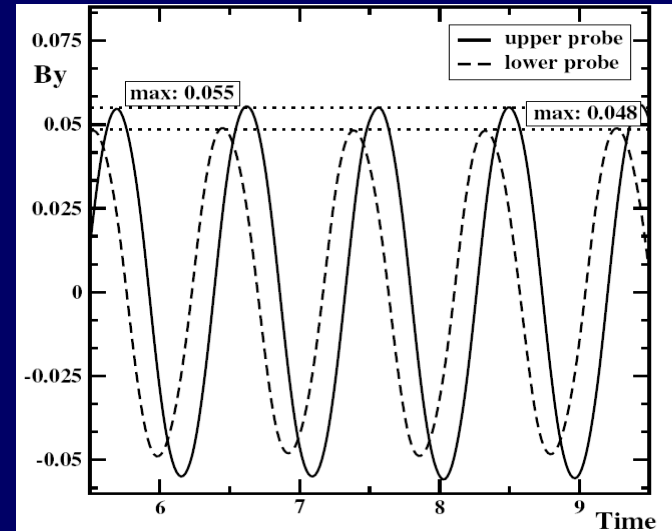
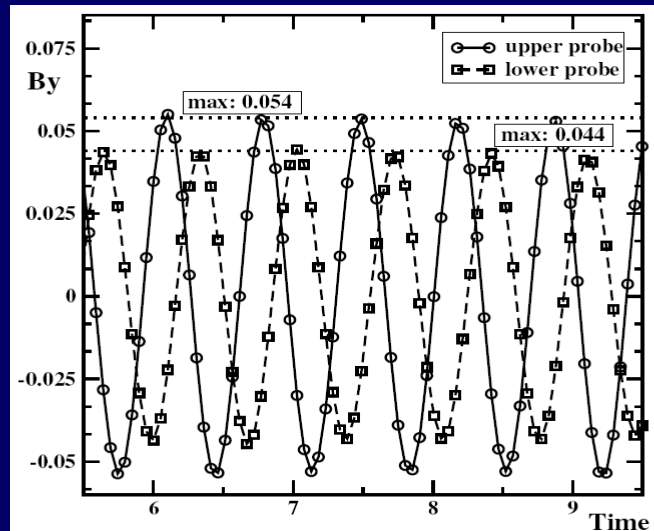
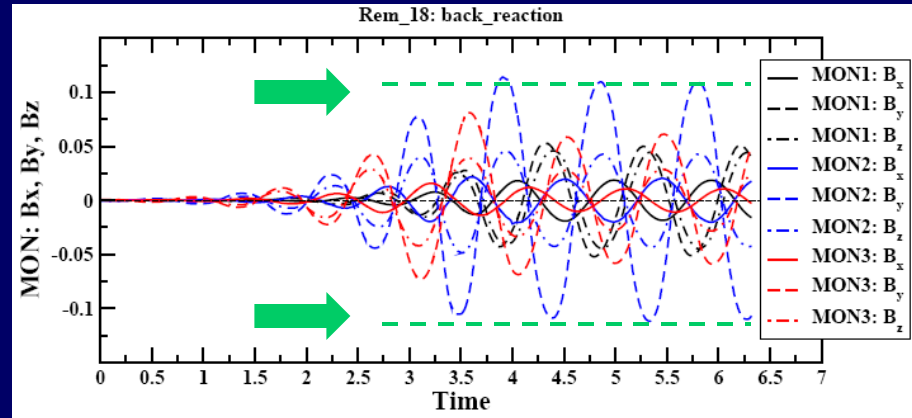
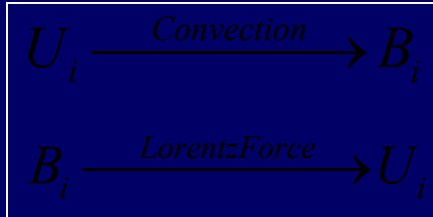
Comparisons with Experiments:



Comparisons with Experiments:



Comparisons with Experiments:



5 December 2007

-experiment-

-simulation-

22

Conclusions:

- **It is demonstrated that two-way coupled turbulent magnetic dynamo in complex geometry was successfully numerically simulated**
- **Application of hybrid T-RANS/DNS approach made it possible to mimic flow and magnetic regimes up to now inaccessible to other simulation techniques (DNS, LES)**
- **It is proved that the action of the hydro-magnetic dynamo in turbulent regime can naturally produce and self-sustain a magnetic field without any external excitation or artificial inputs**

Towards More Efficient Drug Delivery: Blood Flow in Stenotic Arteries Subjected to a Strong Non-Uniform Magnetic Field

5 December 2007

24



Motivation:

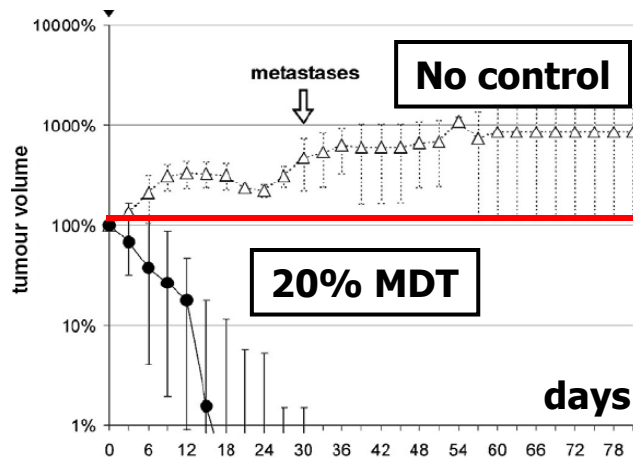
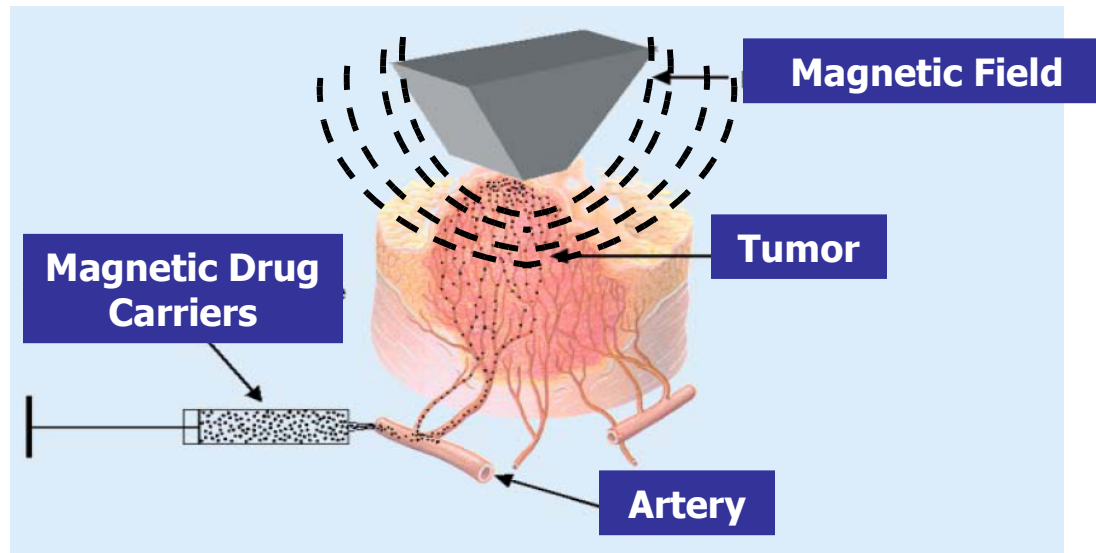
- Ongoing challenge of chemotherapy:
to provide specific delivery of chemotherapeutic agents to their desired targets
with a minimum of systemic side effects
- Locoregional Cancer Treatment with Magnetic Drug Targeting (MDT)
- Mathematical modelling and numerical simulations as a tool for further
advancements of Magnetic Drug Targeting: **Fluid Mechanics** / **Electromagnetism**

Goal:

- To provide insights into fundamental physics of **blood flow** subjected
to **strong external magnetic fields**
- *A priori* personalised parametric studies mimicking individual patient conditions
- Tailoring optimised magnetic fields (strength, gradients, penetrative capabilities)
for bio-medical applications



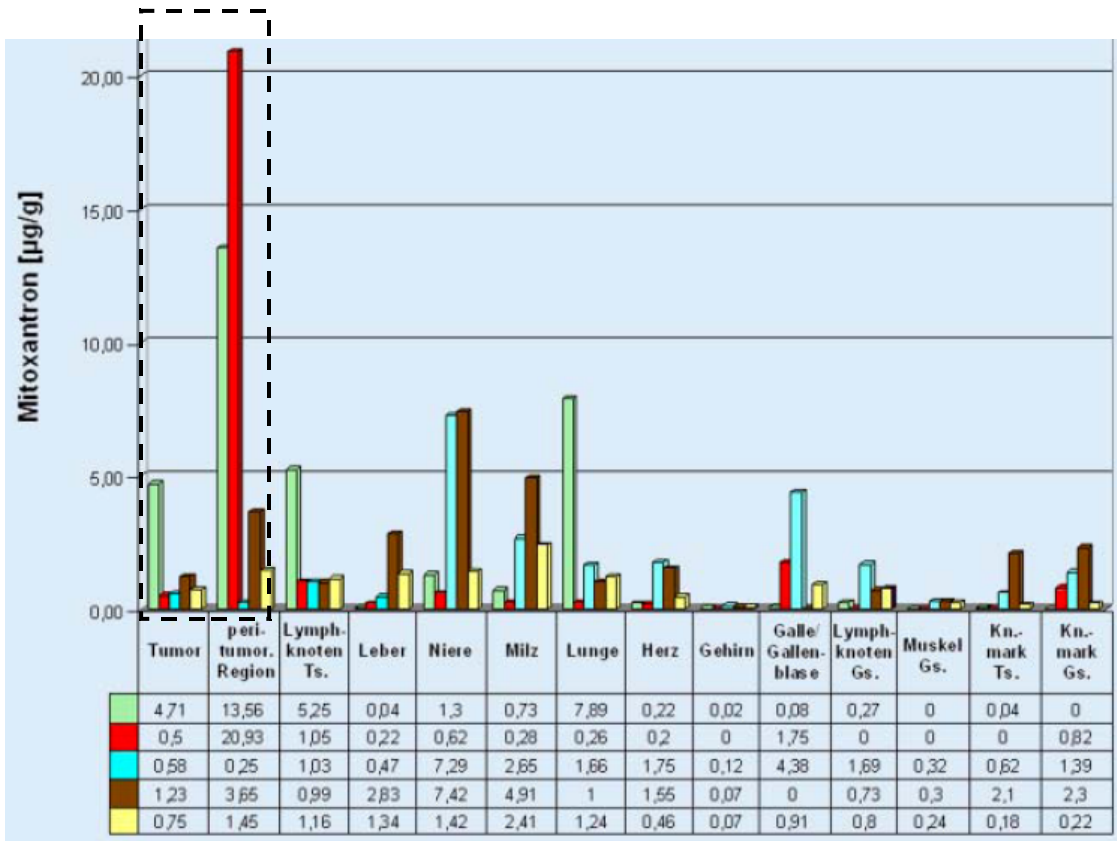
-Principles of local chemotherapy with Magnetic Drug Targeting- Alexiou et al. (2003,2005,2006)



Rabbits with limb tumor 40 days after treatment:
A) 20% of systemic dose with MDT
B) 75% regular systemic dose



-Mitoxantron concentrations 60 min after application: B=0.6 [T]



-B on-

— 20% systemic dosage (FF-M)

— 50% systemic dosage (FF-M)

— 50% systemic dosage (FF-M)

— 100% systemic dosage (FF-M)

-B off-

-Experimental animal studies-
Alexiou et al. (2005)
HNO Vol.53, pp.618-622

Conclusions:
20 – 50 % smaller drug dosage
26 times higher local concentrations



Mathematical Model:

Navier-Stokes/Maxwell's Equations

$$\nabla \cdot \mathbf{V} = 0, \quad \nabla \cdot \mathbf{B} = 0 \quad (1)$$

$$\frac{\partial \mathbf{V}}{\partial t} + (\mathbf{V} \cdot \nabla) \mathbf{V} = \nu \nabla^2 \mathbf{V} + \frac{1}{\rho} \left[-\nabla P + \underbrace{\mathbf{J} \times \mathbf{B}}_{\mathbf{F}^L} + \underbrace{\mu_0 (\mathbf{M} \cdot \nabla) \mathbf{H}}_{\mathbf{F}^M} \right] \quad (2)$$

F^L – Lorentz force
(moving electroconducting fluid through imposed **B**)

$$\nabla \times \mathbf{H} = \mathbf{J}, \quad \nabla \cdot \mathbf{J} = 0, \quad \mathbf{J} = \sigma (\mathbf{E} + \mathbf{U} \times \mathbf{B}) \quad (3)$$

F^M – Magnetization force
(magnetisation response due to non-uniform **B**)



Mathematical Model:

Plasma + Red Blood Cells + White Blood Cells + Platelets = Blood

$6-8 \times 10^{-6} \text{ m}$

$2-4 \times 10^{-6} \text{ m}$

Homogeneous fluid for blood vessels $D > 10^{-4} \text{ m}$, Pedley (1980)

Newtonian or Non-Newtonian fluid?

Shear rates $> 100 \text{ s}^{-1}$

Pedley (1980)

Entire cardiac cycle

30% of cardiac cycle non-Newtonian

Johnston et al. (2004,2006)

Models: Carreau, Walburn-Schneck,
Power Law, Cassau, Generalised Power Law, ...



Mathematical Model:

Magnetisation force modelling

Berkovsky et al. (1993), Odenbach (2002):

$$M = n \cdot m \cdot L(\xi) = n \cdot m \left(\coth \xi - \frac{1}{\xi} \right), \quad \xi = \frac{\mu_0 m H}{\kappa T} \quad (4)$$

Berkovsky et al. (1993), Rosensweig (2002), Tzirtzilakis (2005) (isothermal conditions):

$$M = \chi H \quad (5)$$

FM – Magnetization force
(present: simple, non-isothermal, new model)

Table 1: Properties of the bio-magnetic fluid (blood) used for numerical simulations.

ρ	ν	σ	χ^{oxyg}	χ^{deoxyg}
1050.	4×10^{-6}	0.7 – 0.9	-6.6×10^{-7}	3.5×10^{-6}

???



Mathematical Model:

Magnetic field distributions

Biot-Savart law:

$$B = \frac{\mu_0 I}{2\pi R} \rightarrow B_x = -\mu_0 \sum_{i=1}^N \frac{I_i (y - y_i^c)}{(x - x_i^c)^2 + (y - y_i^c)^2}, \quad B_y = \mu_0 \sum_{i=1}^N \frac{I_i (x - x_i^c)}{(x - x_i^c)^2 + (y - y_i^c)^2} \quad (6)$$

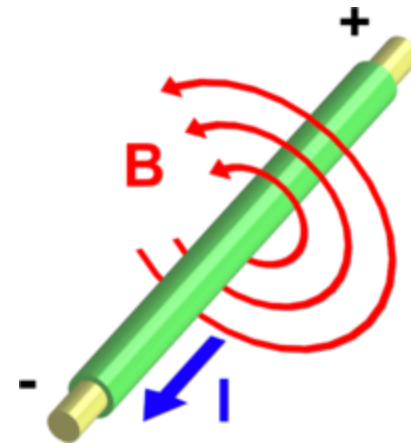
$$B(x, y, z) = \sqrt{B_x^2 + B_y^2 + B_z^2} \quad (7)$$

Lorentz force: ($\mathbf{J} \times \mathbf{B}$)

Ohm's law for moving media + Kirchhoff current continuity condition

$$\mathbf{J} = \sigma (\mathbf{E} + \mathbf{U} \times \mathbf{B})$$

(inductionless assumption)



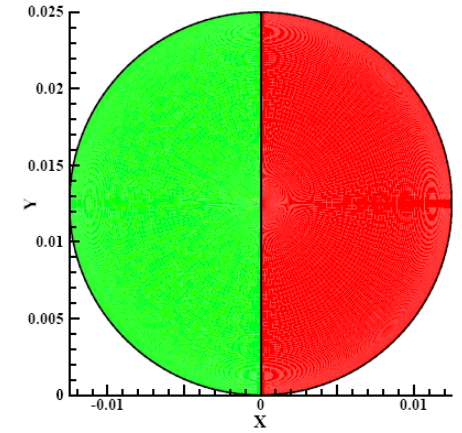
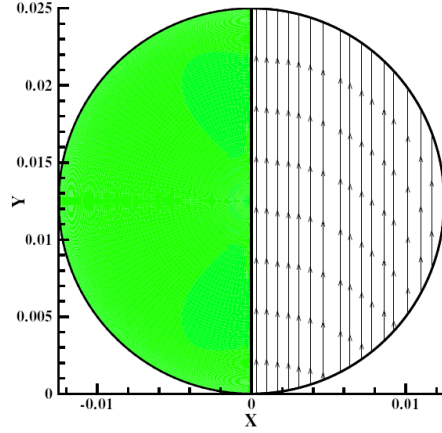
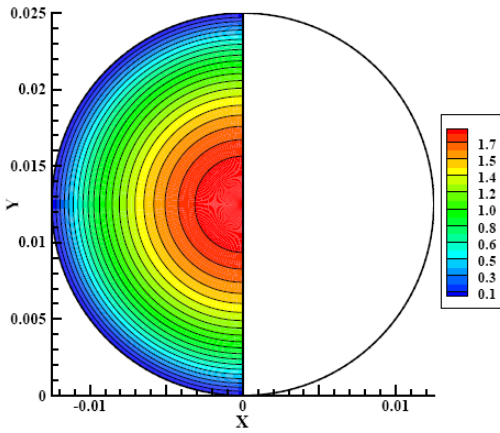
MODEL(S) VALIDATION AND APPLICATIONS:

(I) Steady blood flow in a horizontal cylinder subjected to non-uniform B

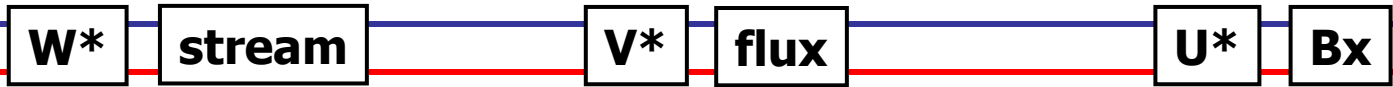
(II) Steady and pulsating blood flow in realistic stenotic arteries

(III) Steady blood flow in stenotic arteries subjected to non-uniform B

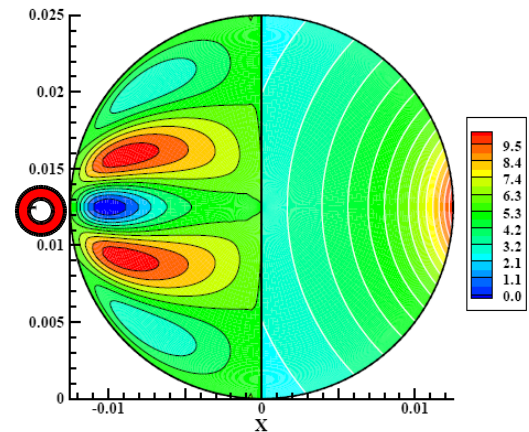
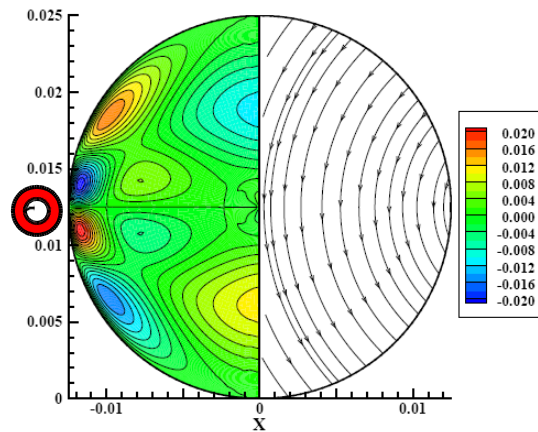
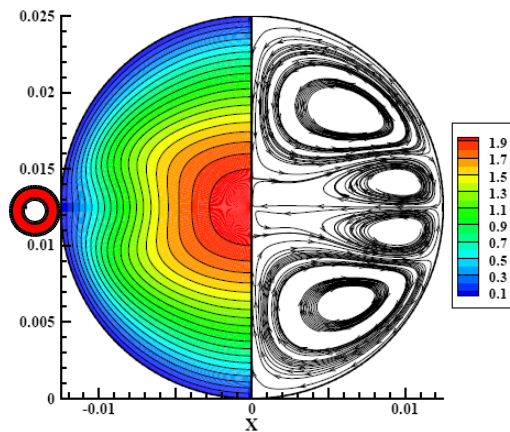


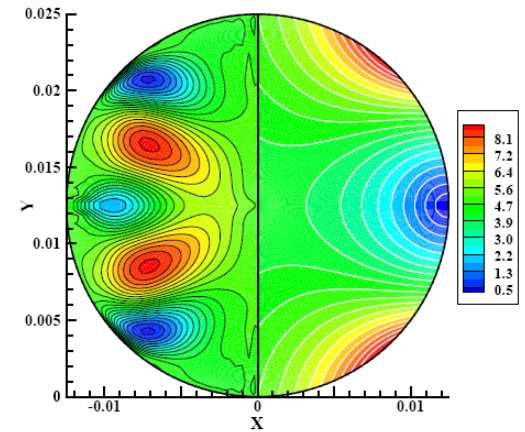
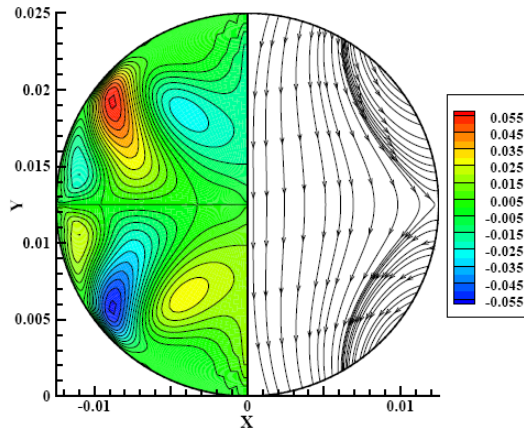
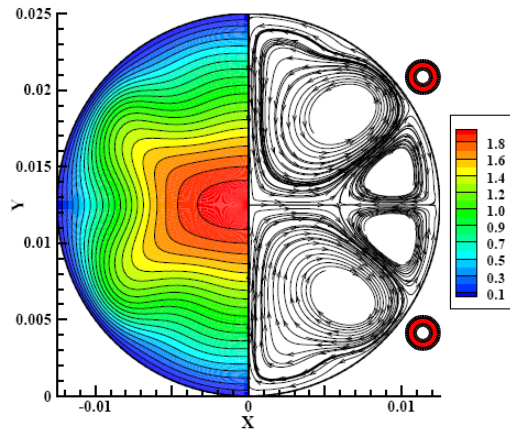


Uniform B



Non-uniform B





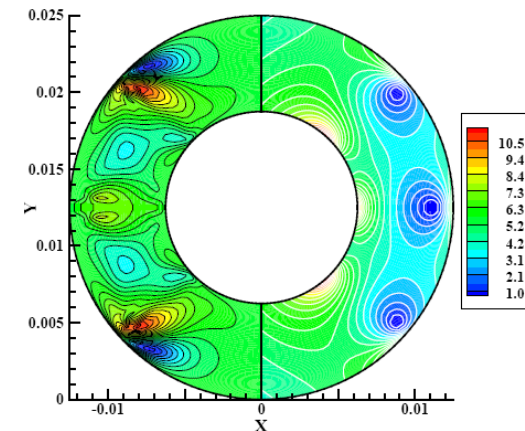
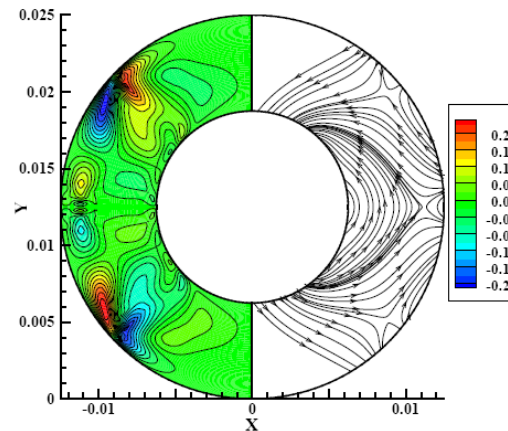
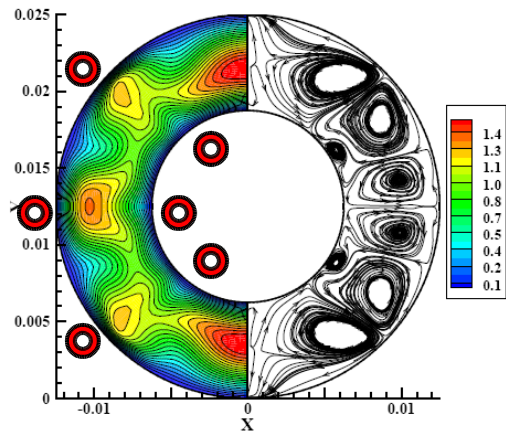
2 sources

W* **stream**

V* **flux**

U* **Bx**

6 sources



MODEL(S) VALIDATION AND APPLICATIONS:

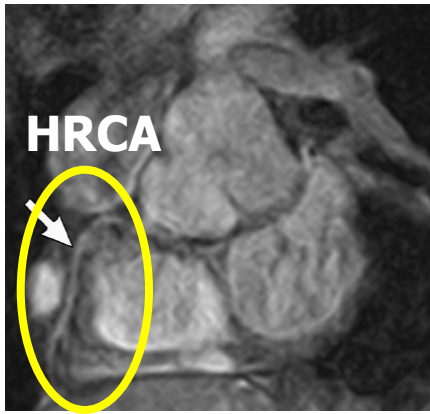
(I) Steady blood flow in a horizontal cylinder subjected to non-uniform B

(II) Steady and pulsating blood flow in realistic stenotic arteries

(III) Steady blood flow in stenotic arteries subjected to non-uniform B

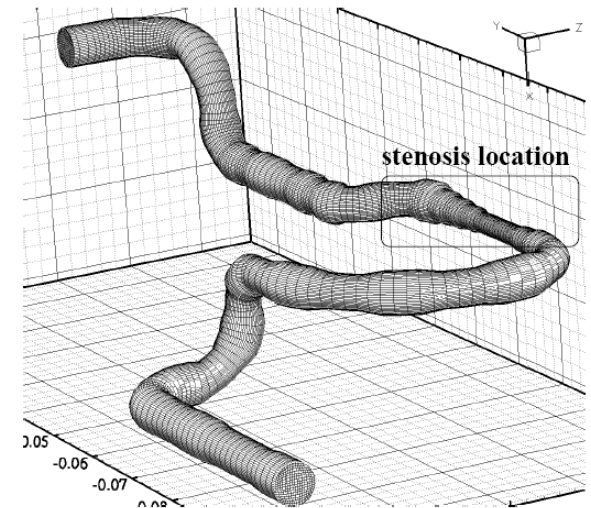
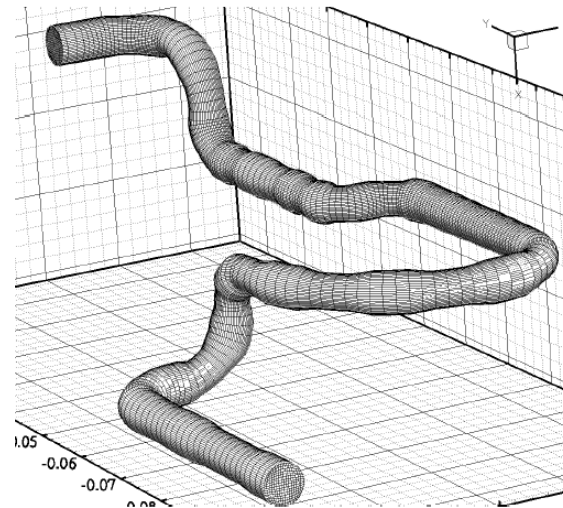
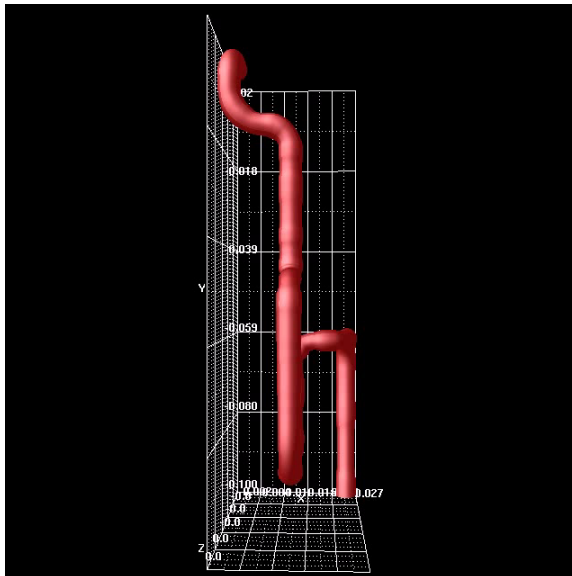


Human right coronary artery (HRCA) → X-ray angiogram to geometrical model

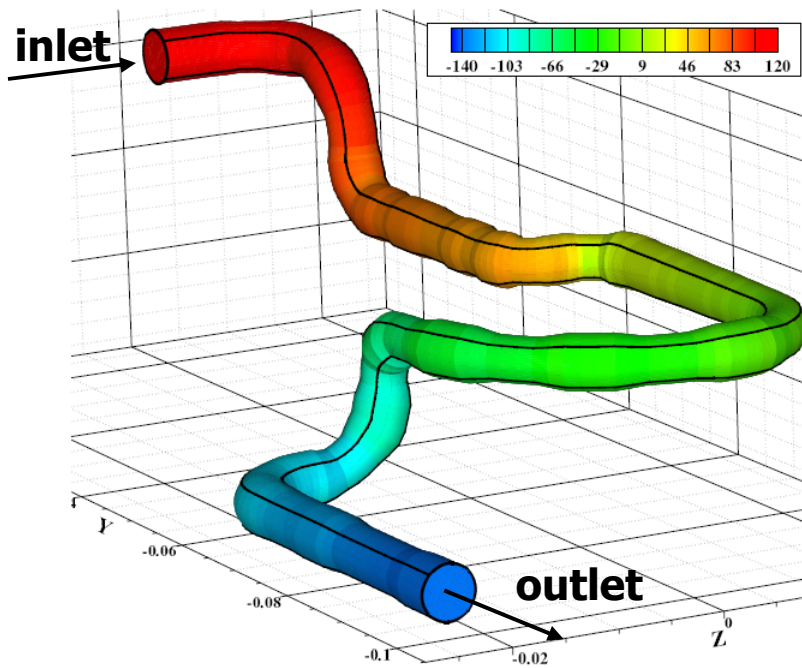


stenosis

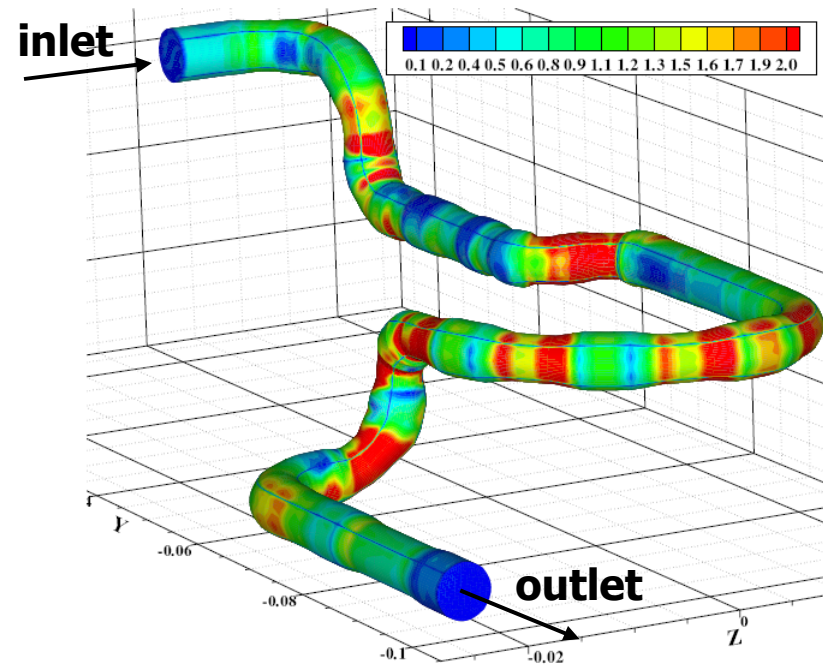
Johnston et al. (2004,2006)
Journal of Biomechanics 37, 39
(steady + transient, no stenosis)



Numerical simulations (healthy artery: 0% stenotic) – steady



-pressure along the vessel wall-

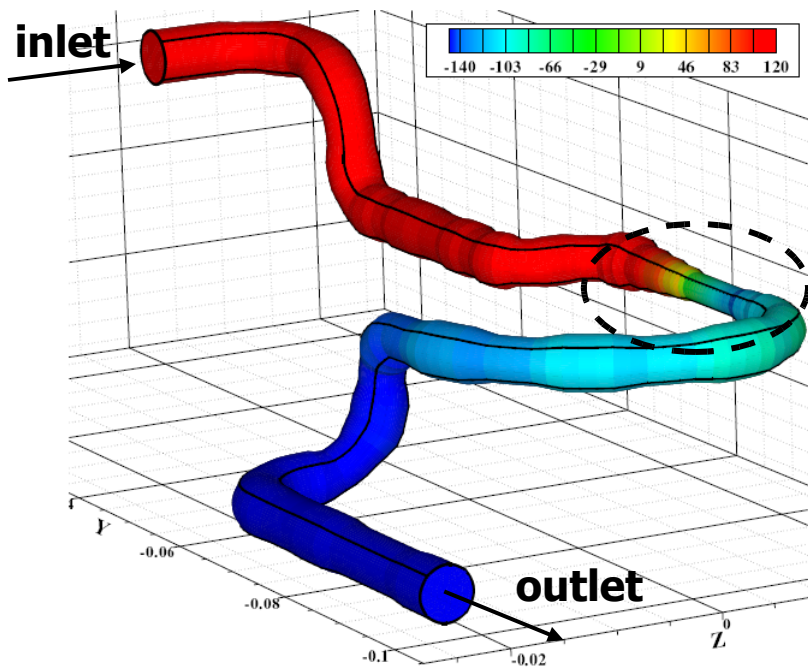


-WSS along the vessel wall-

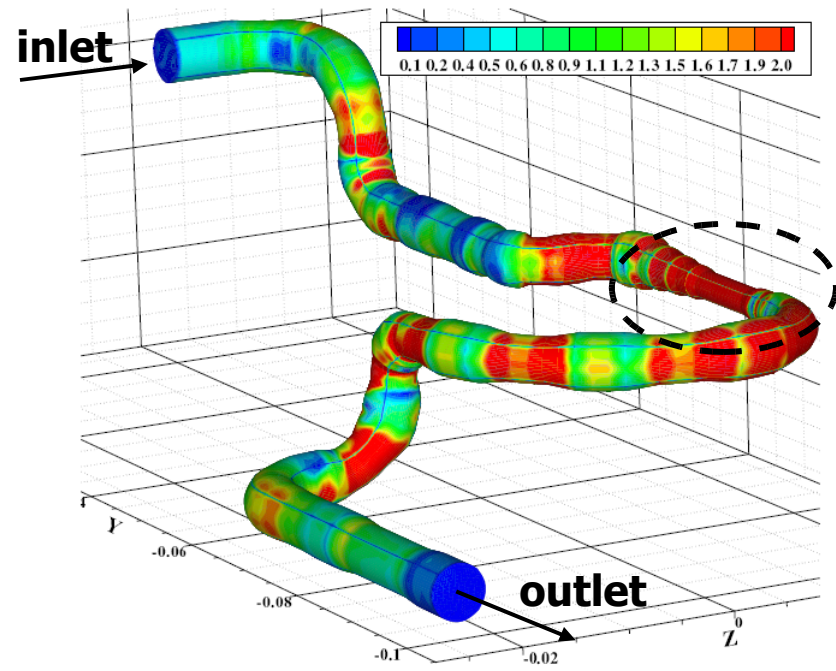
WSS in good agreement with Johnston et al. (2004, 2006): $0 < WSS < 4$ Pa



Numerical simulations (50% stenotic artery) – steady



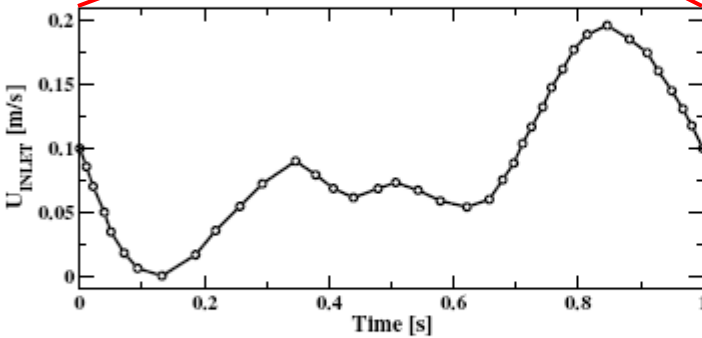
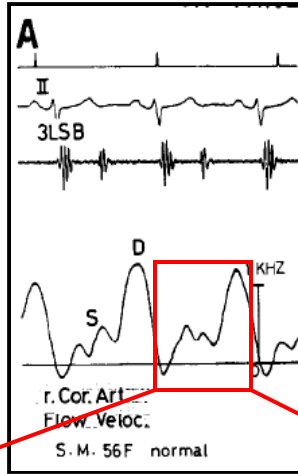
-pressure along the vessel wall-



-WSS along the vessel wall-

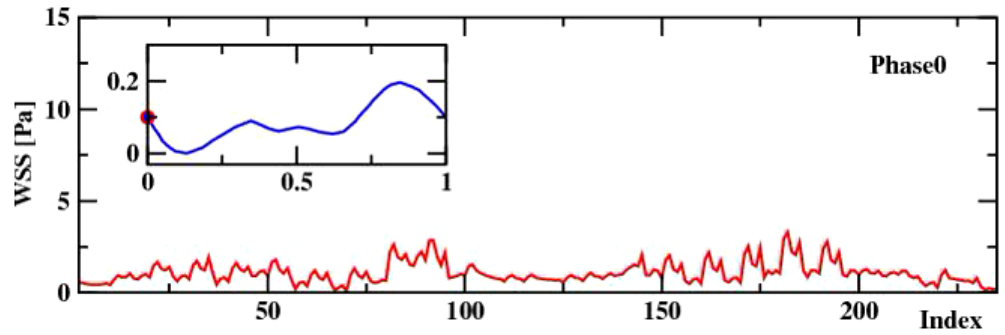


Doppler Flowmeter Catheter recordings:

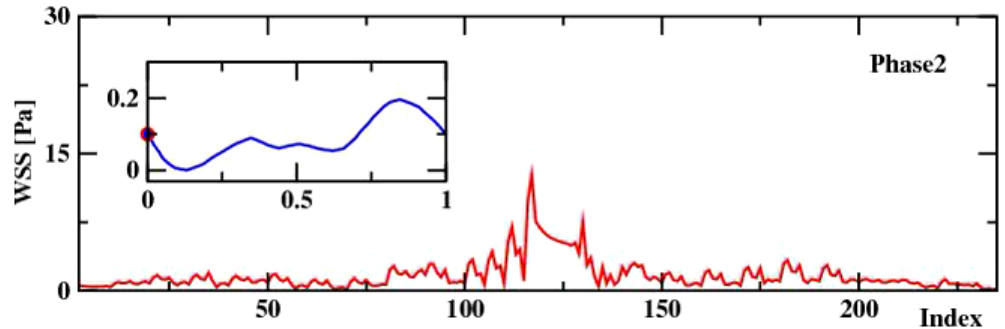


Realistic pulsating cycle:
56 years female
Matsuo et al. (1988)

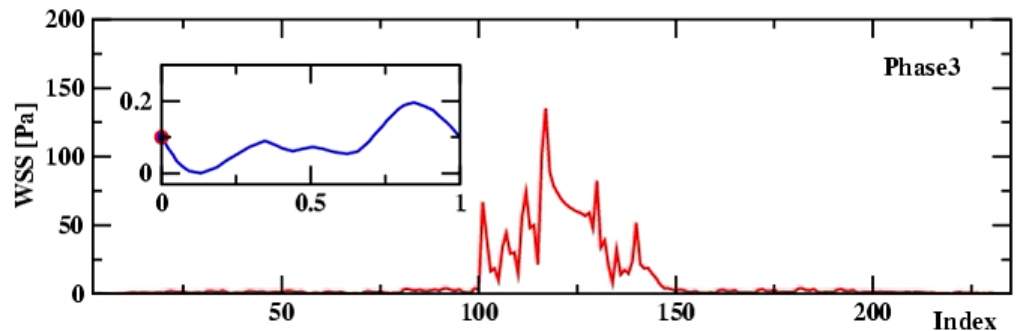
The American Journal of Cardiology 62



-stenosis growth: 0%



-stenosis growth: 50%



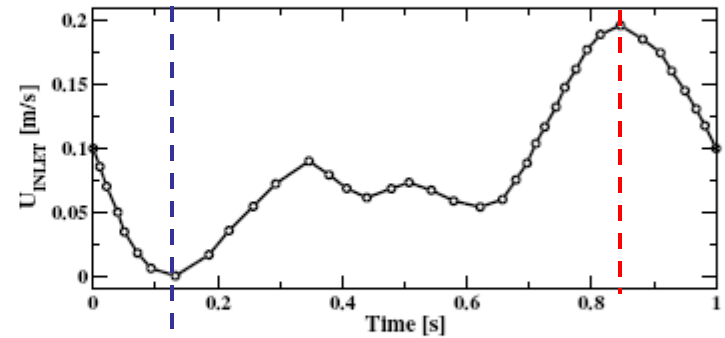
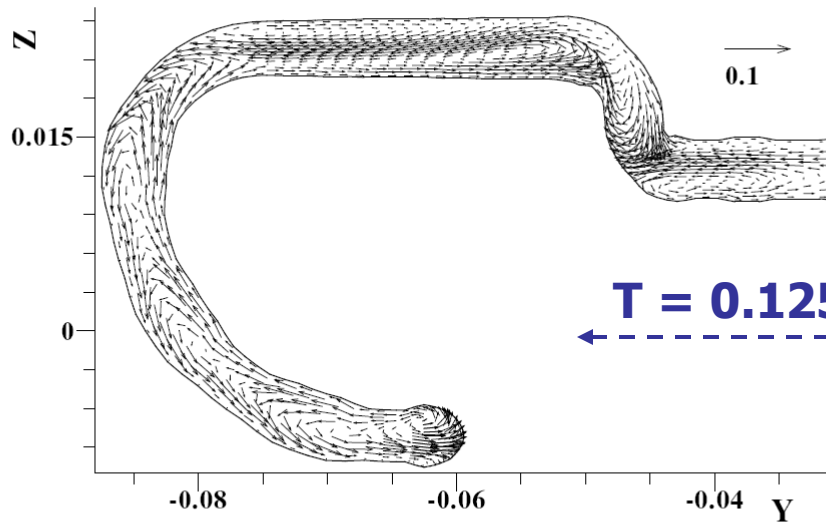
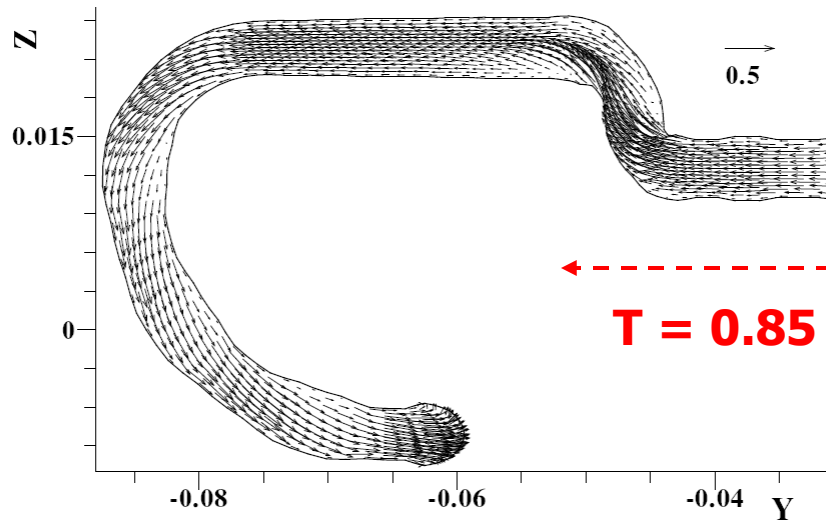
-stenosis growth: 75%

5 December 2007

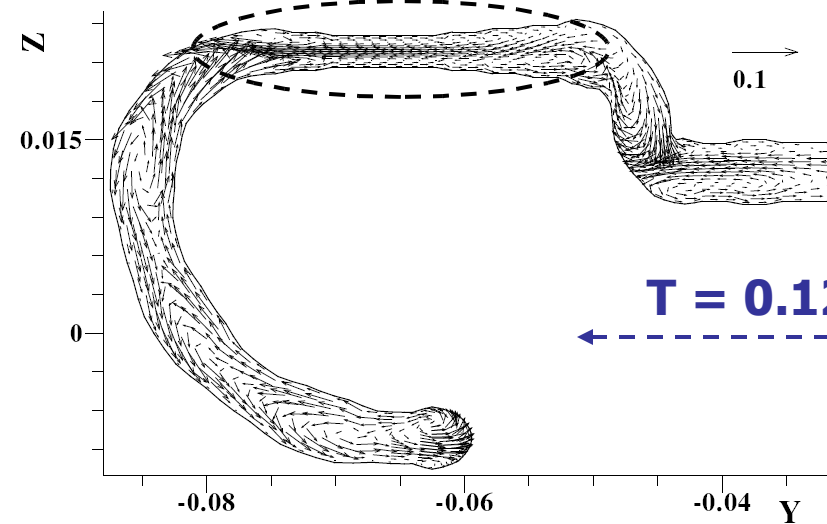
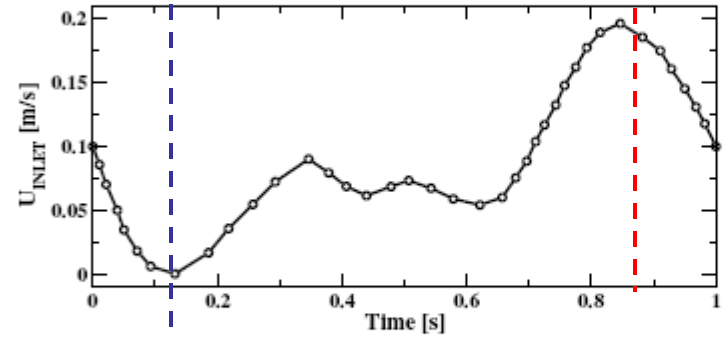
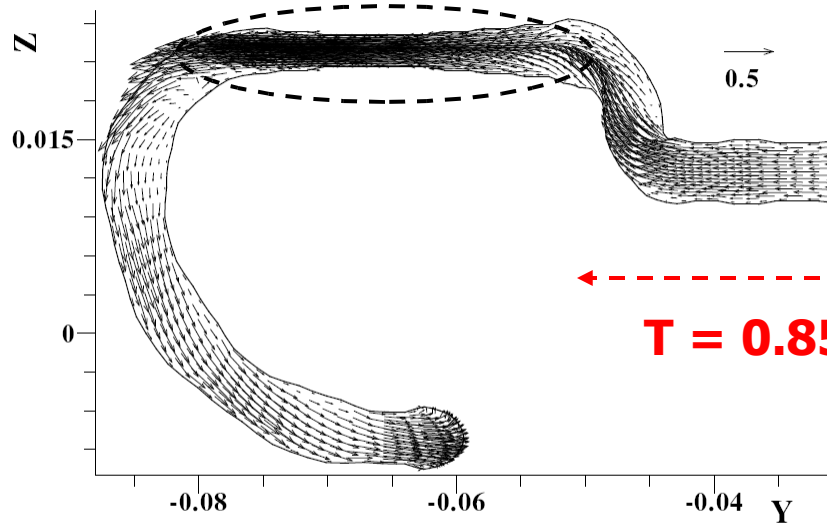
-WSS circumferentially averaged along the arc-length- 39



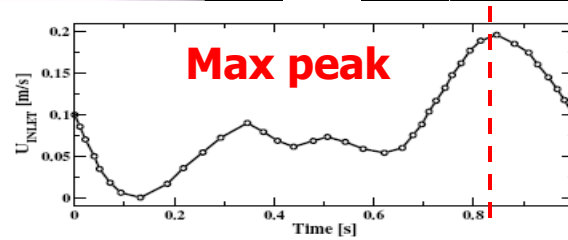
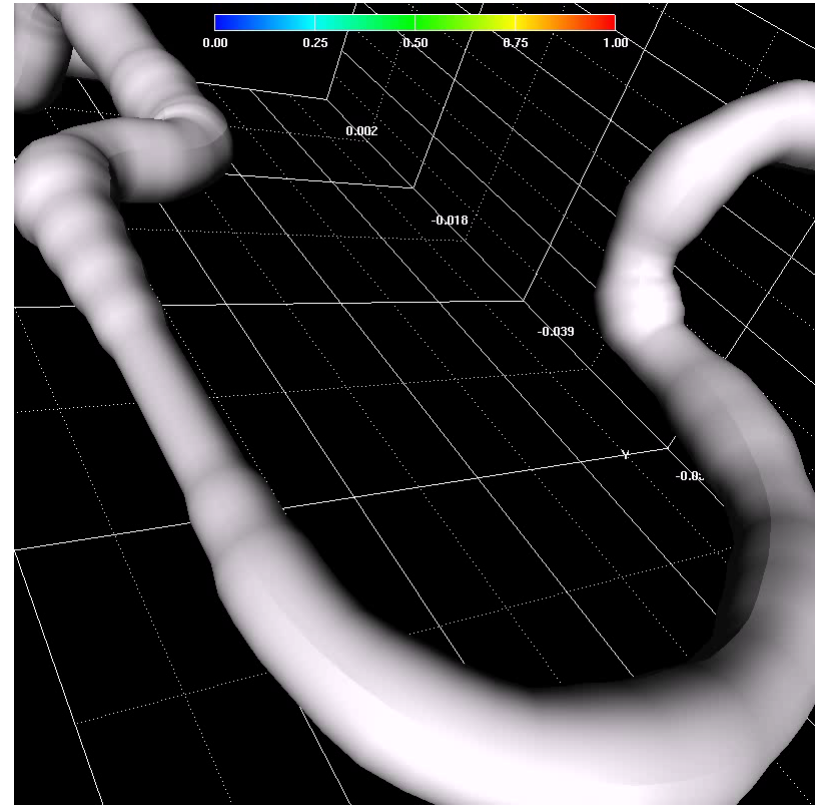
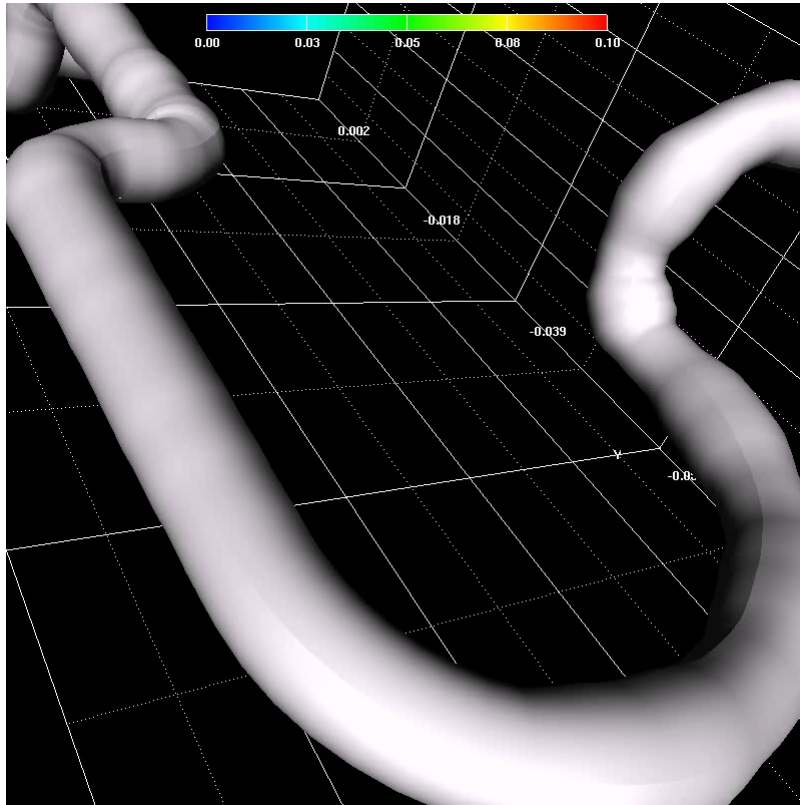
Numerical simulations (healthy artery: 0% stenotic) – pulsating



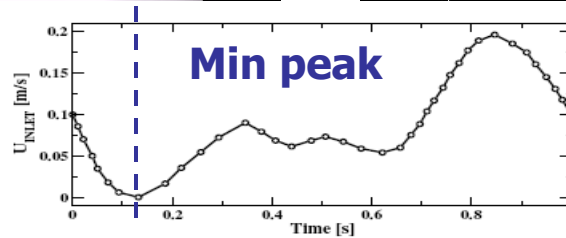
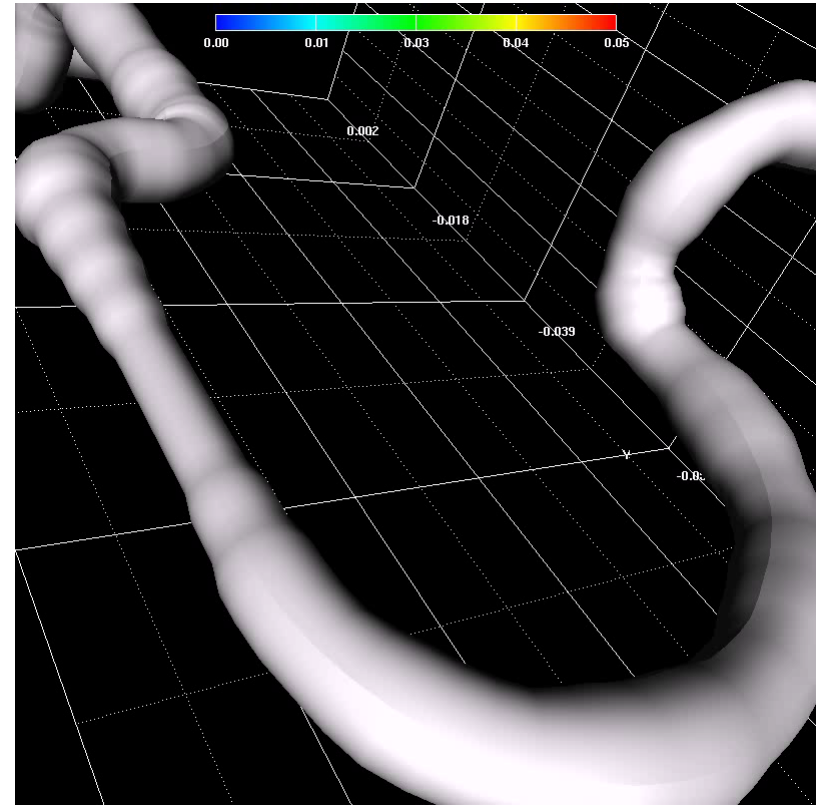
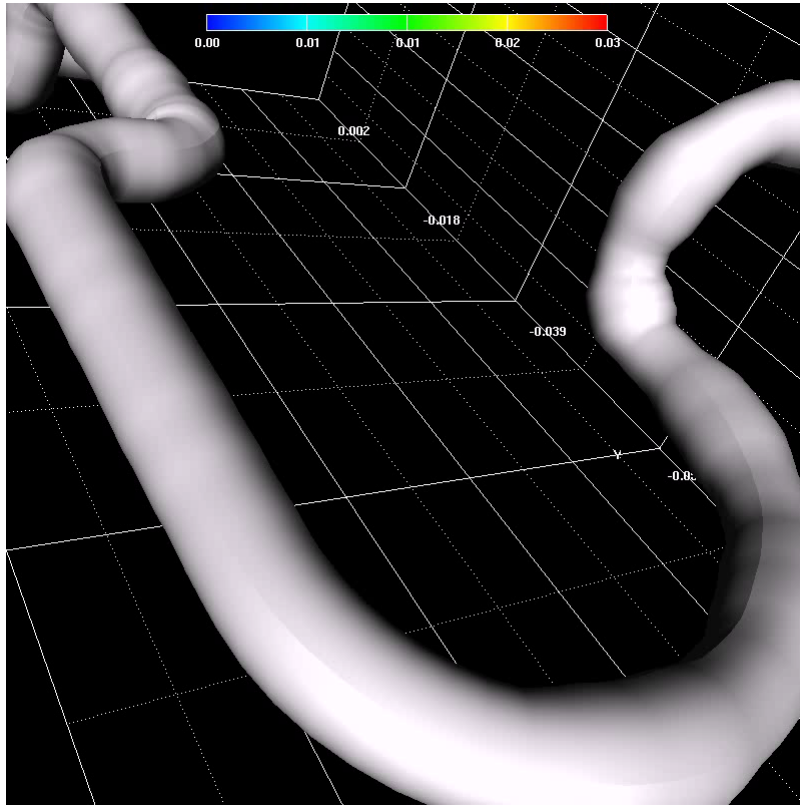
Numerical simulations (50% stenotic artery:) – pulsating



Pulsating simulations (healthy and 50% stenotic RC artery):



Pulsating simulations (healthy and 50% stenotic RC artery):



MODEL(S) VALIDATION AND APPLICATIONS:

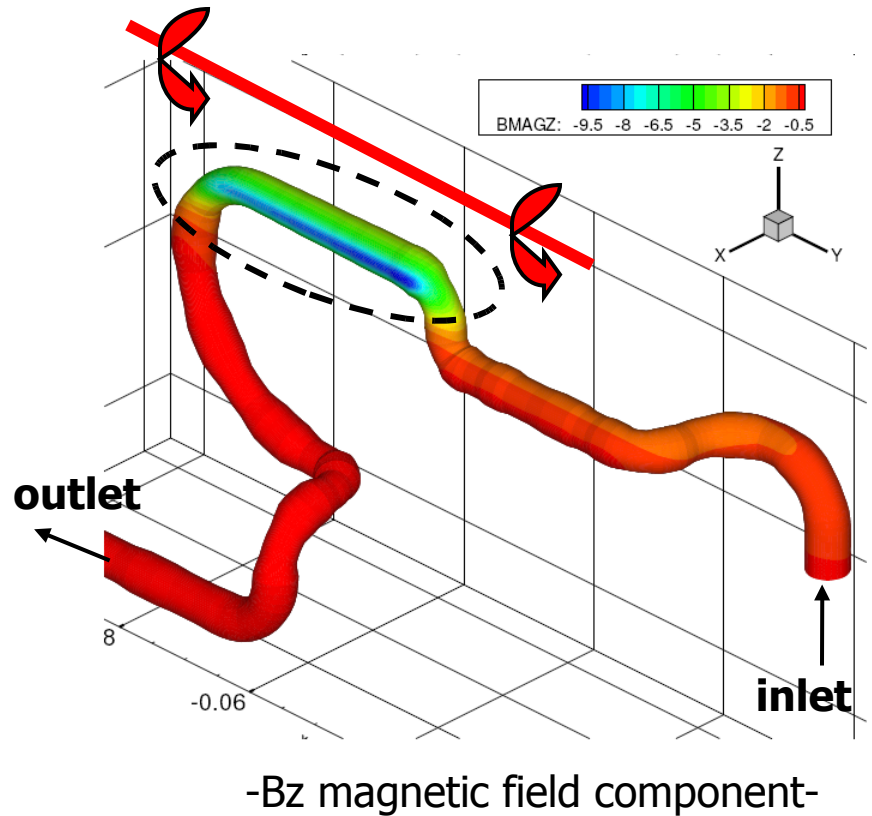
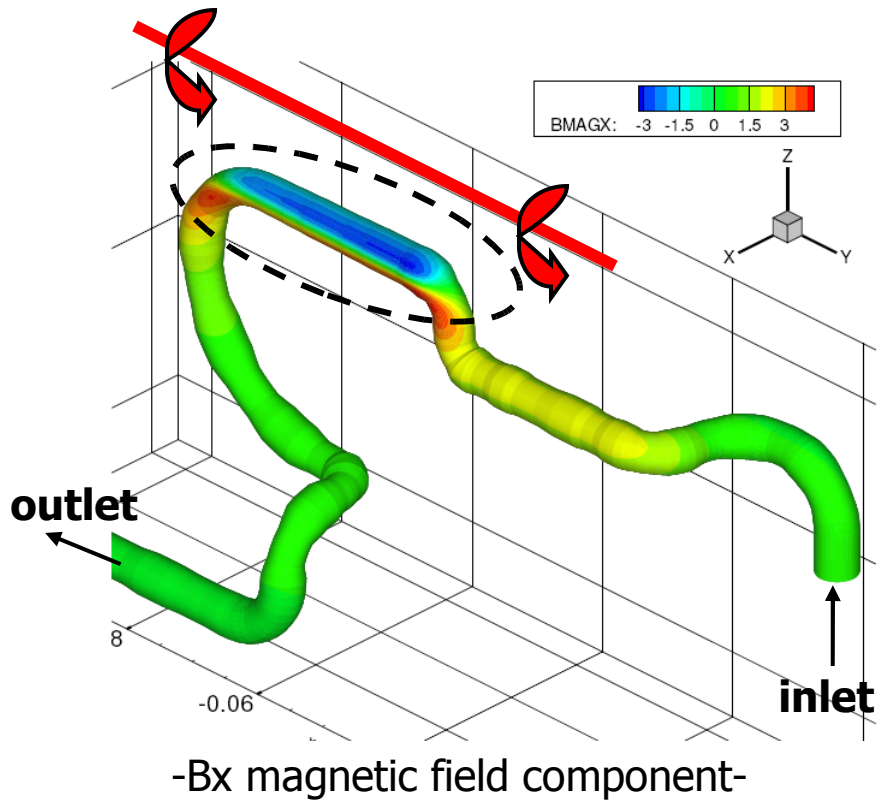
(I) Steady blood flow in a horizontal cylinder subjected to non-uniform B

(II) Steady and pulsating blood flow in realistic stenotic arteries

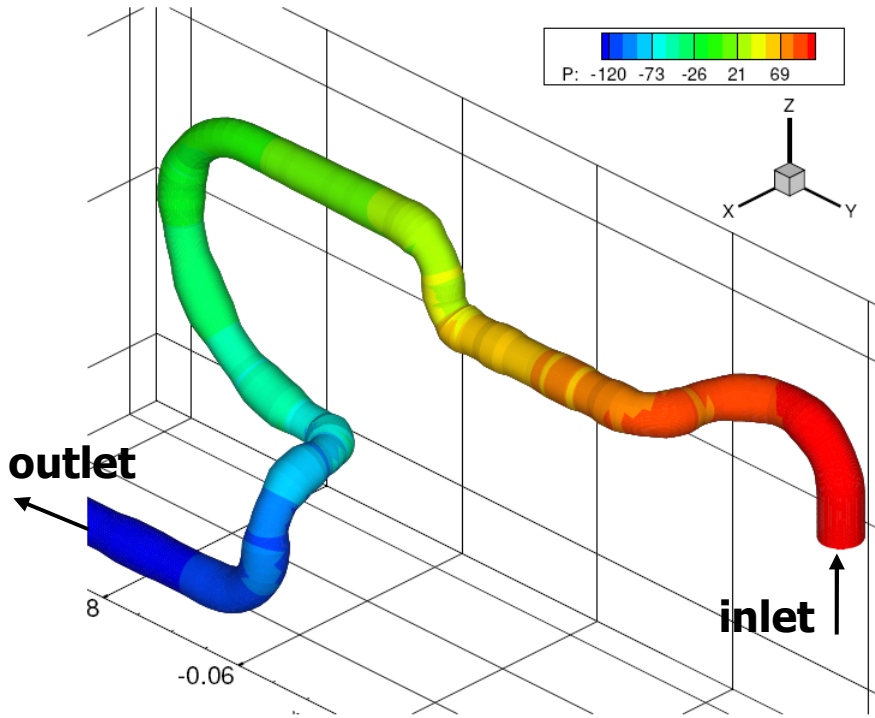
(III) Steady blood flow in stenotic arteries subjected to non-uniform B



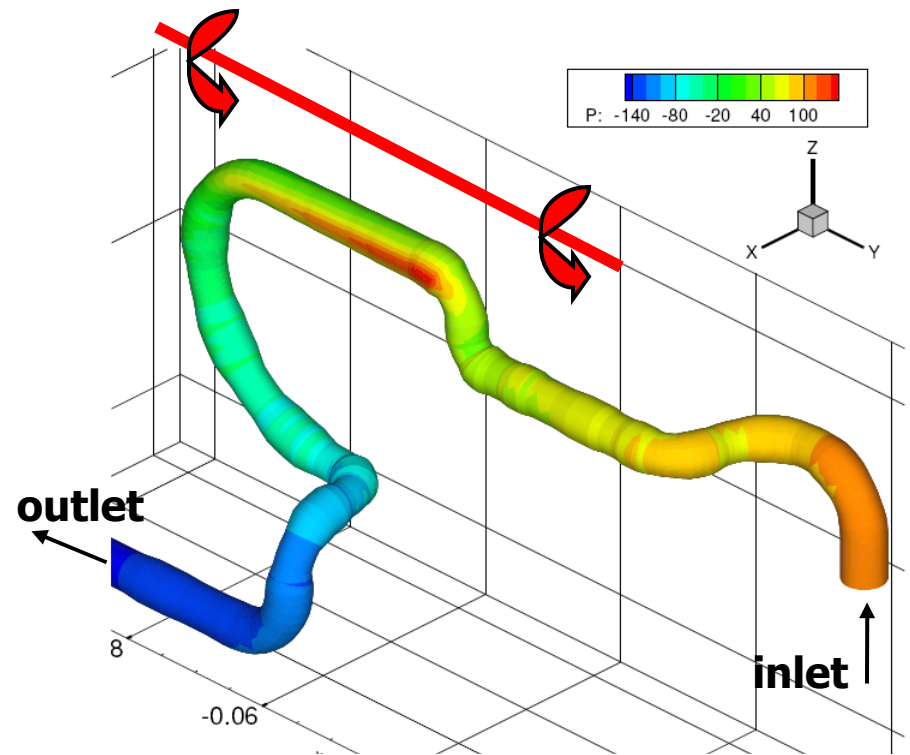
Numerical simulations (healthy artery: 0% stenotic) – steady



Numerical simulations (healthy artery: 0% stenotic) – steady

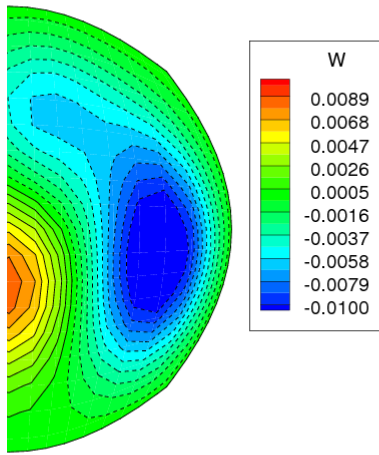


-magnetic field off-



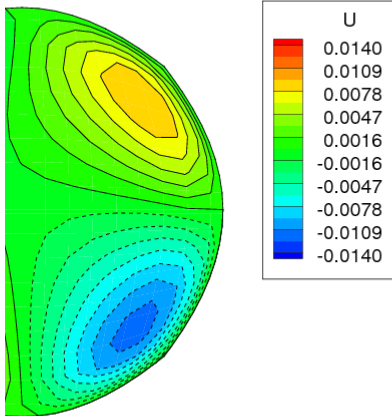
-magnetic field on-



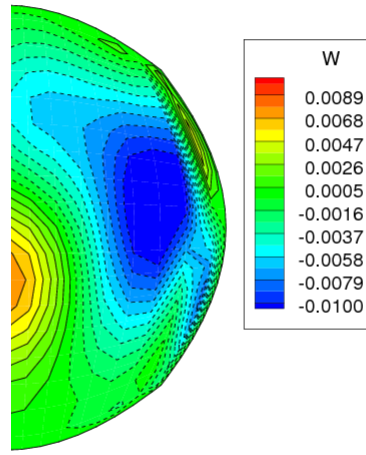


X 0.014

B-off

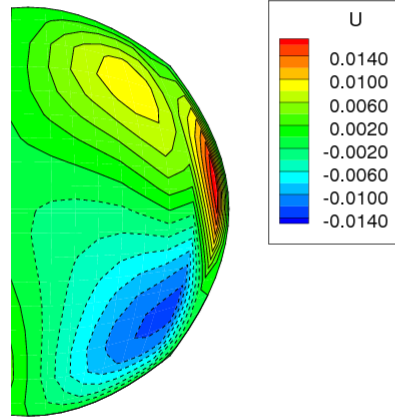


X 0.014

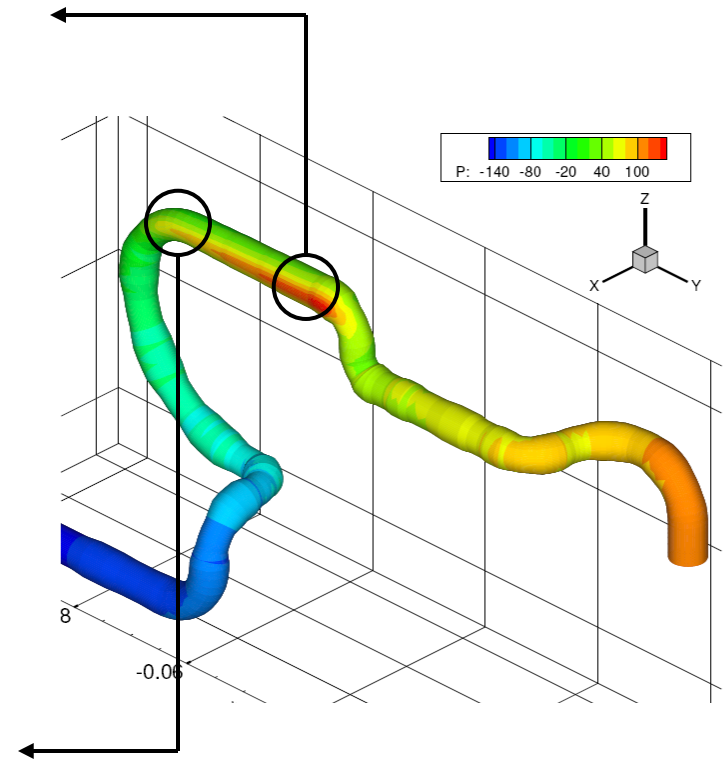


X 0.014

B-on



X 0.014



Conclusions and outlook:

- A comprehensive mathematical model for blood flow subjected to strong non-uniform external magnetic fields derived (fluid flow/electromagnetism interactions)
- An extensive literature survey performed in order to collect physical properties of blood (both dynamical and electrical properties)
- Effects of imposed magnetic field on blood flow patterns clearly demonstrated for steady and pulsating flows in generic and realistic blood vessels geometries

- Future studies: non-linear magnetisation model (fluid-flow/biochemistry coupling)
- Future studies: non-Newtonian effects (pulsating cycles)
- Future studies: multi-branching blood vessels + fluid/structure interactions

